



# Deglaciation and postglacial environmental changes in the Teton Mountain Range recorded at Jenny Lake, Grand Teton National Park, WY



Darren J. Larsen\*, Matthew S. Finkenbinder, Mark B. Abbott, Adam R. Ofstun

Department of Geology and Environmental Science, University of Pittsburgh, Pittsburgh, PA 15260, USA

## ARTICLE INFO

### Article history:

Received 21 September 2015

Received in revised form

19 February 2016

Accepted 22 February 2016

Available online xxx

### Keywords:

Holocene climate change

Lake sediment

Western U.S.

Deglaciation

Grand Teton National Park

Glacier Peak tephra

Teton fault

## ABSTRACT

Sediments contained in lake basins positioned along the eastern front of the Teton Mountain Range preserve a continuous and datable record of deglaciation and postglacial environmental conditions. Here, we develop a multiproxy glacier and paleoenvironmental record using a combination of seismic reflection data and multiple sediment cores recovered from Jenny Lake and other nearby lakes. Age control of Teton lake sediments is established primarily through radiocarbon dating and supported by the presence of two prominent rhyolitic tephra deposits that are geochemically correlated to the widespread Mazama (~7.6 ka) and Glacier Peak (~13.6 ka) tephra layers. Multiple glacier and climate indicators, including sediment accumulation rate, bulk density, clastic sediment concentration and flux, organic matter (concentration, flux,  $\delta^{13}\text{C}$ ,  $\delta^{15}\text{N}$ , and C/N ratios), and biogenic silica, track changes in environmental conditions and landscape development. Sediment accumulation at Jenny Lake began centuries prior to 13.8 ka and cores from three lakes demonstrate that Teton glacier extents were greatly reduced by this time. Persistent ice retreat in Cascade Canyon was slowed by an interval of small glacier activity between ~13.5 and 11.5 ka, prior to the end of glacial lacustrine sedimentation ~11.5 ka. The transition to non-glacial sediments marks the onset of Holocene conditions at Jenny Lake and reflects a shift toward warmer summers, increased vegetation cover, and landscape stability in the Tetons. We discuss the Teton lake sediment records within the context of other regional studies in an effort to construct a comprehensive overview of deglaciation and postglacial environmental conditions at Grand Teton National Park.

© 2016 Elsevier Ltd. All rights reserved.

## 1. Introduction

Mountain ranges in the western U.S. contain a legacy of periodic Quaternary glaciations (e.g. Blackwelder, 1915; Porter et al., 1983; Pierce, 2003 and references therein), which have either directly or indirectly influenced the topography, environmental conditions, and sedimentary systems that exist today (e.g. Hallet et al., 1996; Brozovic et al., 1997; Zhang et al., 2001; Pierce, 2003; Egholm et al., 2009; Foster et al., 2010; Mitchell and Humphries, 2015). These landscapes are characterized by relatively high environmental gradients and are considered particularly sensitive to external disturbances related to climate change and human impacts (Beniston, 2003; Settele et al., 2014). For example, recent

atmospheric warming, dryer conditions, and human activity in mountainous regions of the western U.S. have led to numerous environmental changes, including increased glacier recession (Arendt et al., 2002; Gardner et al., 2013), wildfire occurrence (Westerling et al., 2006), and ecological shifts (Walther et al., 2002), and both decreased alpine snowpack (Mote et al., 2005) and variable water resources (Nelson et al., 2011). Reconstructions of past mountain environments derived from sedimentary deposits are important for placing such changes within the context of longer-term geomorphic and ecologic development, and may improve projections of future changes and the efficacy of natural resource management. Here, we target sediments contained in glacially scoured lake basins at Grand Teton National Park, WY to reconstruct the timing and pattern of deglaciation and subsequent (postglacial) environmental history of the Teton Mountain Range.

The Teton Range in northwest Wyoming is a rectangular (~65 km by ~15 km; roughly north-south trending) fault-block

\* Corresponding author.

E-mail address: [djlarsen@pitt.edu](mailto:djlarsen@pitt.edu) (D.J. Larsen).

mountain range located within the Middle Rocky Mountain physiographic province (Fenneman, 1931, Fig. 1). The bedrock geology of the Range consists primarily of a Precambrian crystalline core (e.g. quartz monzonite and gneisses) unconformably overlain by a sequence of westward-tilting Cambrian and Paleozoic sedimentary units (Love et al., 1992, 2003; Pierce and Good, 1992; Smith et al., 1993). During the most recent (Pinedale) glaciation, the Tetons and adjacent Yellowstone region contained one of the largest mountain glacier ice complexes in the western U.S. (Porter et al., 1983) and glacier deposits (e.g. moraines, till, outwash) are

common, particularly in the broad low-lying basins that flank both sides of the range (Fig. 1). The dramatic topography and geomorphic asymmetry of the Tetons is attributed to uplift along the Teton fault, a major range-bounding, eastward-dipping normal fault that extends for ~70 km along the base of the mountains (Love et al., 1992, 2003; Smith et al., 1993; Byrd, 1994; Byrd et al., 1994). Well-preserved fault scarps up to ~30 m tall displace Pinedale-age glacier deposits and provide evidence for recent fault activity (Fig. 1; Smith et al., 1993; Machette et al., 2001; Foster et al., 2010; Thackray and Staley, 2014). The active tectonic setting and glacial

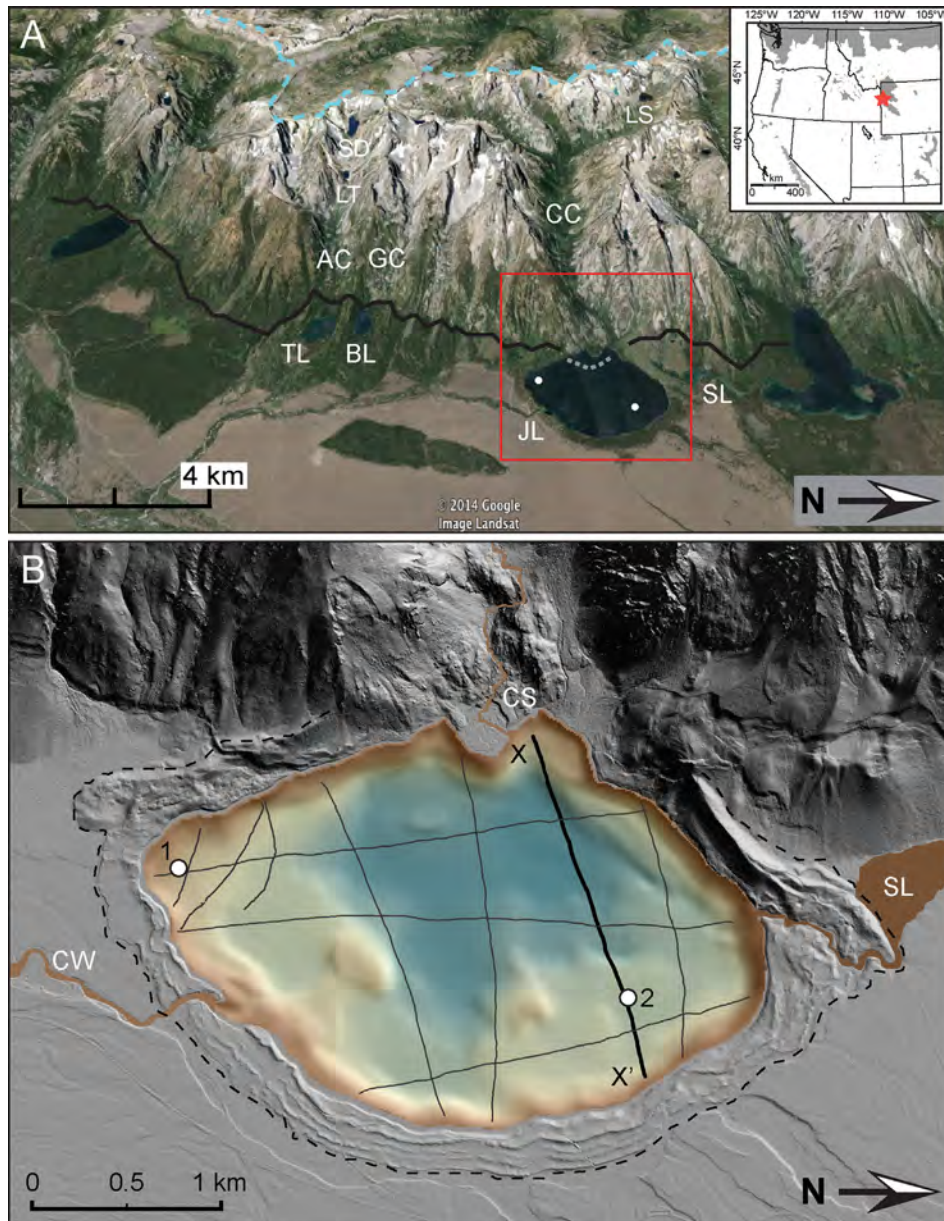


**Fig. 1.** Overview maps and geologic setting of study region. (A) Oblique aerial view of eastern flank of the Teton Mountain Range. Note the series of glacially carved valleys and moraine-impounded piedmont lakes located at their base. The three valleys and their respective lakes mentioned in the text are Cascade Canyon (CC), Jenny Lake (JL), Lake Solitude (LS), Garnet Canyon (GC), Bradley Lake (BL), Avalanche Canyon (AC), Taggart Lake (TL), Lake Taminah (LT), and Snowdrift Lake (SD). The Teton fault trace is marked with a black line (approximate location of the fault trace below Jenny Lake is marked by dashed grey line). The drainage divide is located near the top of the frame (dashed blue line). Inset map highlights location of Tetons (star) on map of western U.S. glaciers during Pinedale time (from Porter et al., 1983). Red square delineates area enlarged in panel B. (B) Lidar hillshade map of area surrounding Jenny Lake highlighting the mouth of Cascade Canyon and the position of the lake behind a Pinedale-age moraine complex (dashed black line). The locations of seismic profiles are shown along with lake bathymetry (cooler colors represent greater water depth; raster map provided courtesy of NPS) and core sites JEN13-1 and JEN13-2 (white dots). Seismic profile X-X' is presented in Fig. 2. Inflows to Jenny Lake are Cascade Creek (CS), which drains Cascade Canyon, and a stream that emanates from String Lake (SL) to the north. Lake outflow occurs through Cottonwood Creek (CW) to the south. (For interpretation of the references to colour in this figure legend, the reader is referred to the web version of this article.)

geomorphic history of the Tetons have created a series of roughly parallel glacial valleys carved into the steep eastern front of the range (Fig. 1). Many of the valleys drain into moraine-dammed piedmont lakes positioned along the Range front. Sediment fill in each lake marks the timing of glacier retreat at the end of the Pinedale glaciation and preserves a continuous and datable record of subsequent upstream glacier activity and landscape evolution related to environmental conditions in the catchment.

We develop an integrated record of glacier variations and environmental changes using a combination of seismic profiles and sediment cores from Jenny Lake, and supportive information contained in cores from nearby Taggart and Bradley Lakes (Fig. 1). Numerous previous studies have investigated the tectonic (Roberts and Burbank, 1993; Smith et al., 1993; Byrd et al., 1994; Love et al., 2003; Hampel et al., 2007; Hampel and Hetzel, 2008; Pickering White et al., 2009), geomorphologic (Pierce, 2003; Foster et al., 2008, 2010; Tranel et al., 2011, 2015), glacier geologic (Pierce and Good, 1992; Love et al., 2003; Licciardi and Pierce, 2008; Pierce et al., 2011), and ecologic (Whitlock, 1993; Whitlock and Bartlein, 1993; Millspaugh et al., 2004; Whitlock et al., 2008, 2012; Krause and Whitlock, 2013; Krause et al., 2015) history of the Tetons and nearby Yellowstone region. We discuss the Jenny Lake sediment record within the context of these and other relevant studies in an effort to construct a comprehensive overview of deglaciation and postglacial environmental conditions in the Tetons.

## 2. Geologic setting

Jenny Lake (43.76 N, 110.73 W; 2070 m asl) is a large piedmont lake located at the base of Cascade Canyon in the central part of the Teton Range (Fig. 1). The lake has an area of ~5 km<sup>2</sup>, a maximum depth of ~73 m, and an average depth of ~43 m. Two main inflows are Cascade Creek, which drains Cascade Canyon, and a stream that emanates from String Lake to the north (Fig. 1). Catchment areas of the two inflows are each ~45 km<sup>2</sup> and they span the full elevation gradient of the Tetons, reaching altitudes of nearly 4200 m asl. Jenny Lake is classified as slightly oligotrophic (Dustin and Miller, 2001). Mean annual temperature and precipitation measured 10 km south of Jenny Lake at Moose, WY (~1970 m asl) are 3.1 °C and ~550 mm, respectively (Fig. S1; NOAA; reference period: 1981–2010 CE). Precipitation is dominated by winter snowfall (Fig. S1), particularly at higher elevations within the catchment. Cold winters and thick snowpack result in prolonged lake ice cover, which commonly persists from November to May. Soils in the catchment are generally thin and poorly developed. Modern vegetation varies according to moisture availability and elevation, and ranges from sagebrush steppe communities at low elevations to alpine tundra (Shaw, 2000). Mixed conifer forests cover the moraines immediately surrounding Jenny Lake and occur in patches in Cascade Canyon, primarily in areas of low slope and those protected from mass movement events. Hillslope failures affect large portions of the canyon and are considered to be important agents of erosion, sediment transport, and long-term landscape evolution (Foster et al., 2010; Marston et al., 2011; Tranel et al., 2015).

The primary sediment source to Jenny Lake is via Cascade Creek. Sediment transported by this stream has created a small delta at the mouth of Cascade Canyon along the western lakeshore (Fig. 1). The absence of a delta to the north indicates that String Lake is presently not an important source of sediment. Lake outflow occurs to the south via Cottonwood Creek, a broad shallow overflow channel that transects a relatively subdued segment of the impounding moraine complex. Relict meltwater channels and outwash deposits from the Yellowstone glacial system are clearly visible in Lidar (light detection and ranging) data and suggest

drainage patterns in the vicinity were substantially different during Pinedale times (e.g. Pierce and Good, 1992; Licciardi and Pierce, 2008, Fig. 1).

Similar to other piedmont lakes in the Tetons, Jenny Lake formed in the late Pleistocene following regional deglaciation (Love et al., 2003). The lake occupies a terminal basin excavated by a major valley glacier during its Pinedale advance and was developed in part by outwash buildup outside the area covered by the glacier terminus (e.g. Pierce and Good, 1992). The relatively narrow terminal moraine complex encircling the lake contains multiple closely nested ridges and likely contains outer segments that are buried by outwash (Licciardi and Pierce, 2008, Fig. 1). The height of the inner moraine crest above the lake surface varies along the lake perimeter from a maximum of ~200 m near the canyon mouth, an average of ~25 m along the eastern shore, and minimum of ~4 m on the southern margin. Bathymetric data indicate the steep backslope of the inner moraine continues below the lake surface before intercepting a relatively flat shelf that surrounds a central over-deepened basin (Fig. 1).

## 3. Methods

### 3.1. Seismic survey, sediment cores, and sedimentary indicators

A seismic survey of Jenny Lake was conducted to map the spatial distribution of sediment and to identify optimal coring locations (Fig. 1). The survey was performed in a gridded manner using an EdgeTech 3100 compressed high intensity radar pulse (CHIRP) sub-bottom profiler operated at frequencies of 4–20 kHz. Sediment thickness was estimated using the velocity of sound in freshwater (~1500 m s<sup>-1</sup>). Two core sites (JEN13-1 and JEN13-2; Fig. 1; Table 1) were selected for their locations in the distal shelf region of the basin, where seismic profiles indicate regular undisturbed horizontal stratigraphy and sediment deposition occurs predominantly through suspension settling. The influences of past disturbances (e.g. landslides, sediment gravity flows, flood events) at these sites were considered minimal. Multiple sediment cores were collected from both locations using a percussion-driven piston corer deployed on cables from the frozen lake surface in April 2013. Sediment cores were also collected from nearby Bradley and Taggart Lakes using the same methods (Fig. 1). All cores were packaged in the field and transported to the University of Wyoming and the National Lacustrine Core Facility (LacCore) at University of Minnesota for initial core processing and description. Core sections were split longitudinally and core halves photographed using a Geotek Geoscan line-scan core imager. The cores were subsequently transported to the Department of Geology and Environmental Science at the University of Pittsburgh for sub-sampling and additional analyses.

We measured sediment dry bulk density on all cores at continuous 1 cm intervals by weighing 1 cm<sup>3</sup> samples after drying in a low temperature oven (~60 °C). Total organic matter content (TOM) was measured at continuous 1 cm intervals using loss on ignition (LOI) at 550 °C for 4 h following Heiri et al. (2001). Samples for total organic carbon (TOC), total nitrogen (TN), and stable carbon and nitrogen isotopes ( $\delta^{13}\text{C}$  and  $\delta^{15}\text{N}$ ), were taken from core JEN13-1C at continuous 2 cm intervals ( $n = 127$ ) and processed at the University of California, Davis using a PDZ Europa ANCA-GSL elemental analyzer interfaced with a PDZ Europa 20-20 isotope ratio mass spectrometer (IRMS). Prior to analyses, samples were pretreated with 1 M HCl and rinsed back to neutral with purified water. Samples were then freeze dried, homogenized, and combusted at 1020 °C, and N<sub>2</sub> and CO gas were separated on a Carbo-sieve GC column (65 °C, 65 mL/min) before entering the continuous-flow IRMS for isotope measurements. The  $\delta^{13}\text{C}$  and  $\delta^{15}\text{N}$  values are reported as ‰ values relative to Vienna Pee Dee

**Table 1**  
Teton lakes sediment core metadata.

Lake name	Core ID	Latitude	Longitude	Water depth (m)	Spliced core length (m)	Approx. core age (cal yr BP)
Jenny	JEN13-1C	43.75054	110.73428	25.4	2.56	14,200
Jenny	JEN13-2A	43.77172	110.72578	45.2	1.06	9200
Jenny	JEN13-2B	43.77172	110.72578	45.2	1.49	11,400
Jenny	JEN13-2D	43.77172	110.72578	45.2	1.56	11,500
Jenny	JEN13-2E	43.77172	110.72578	45.2	2.09	13,900
Taggart	TAG13-2A	43.70492	110.75282	6.4	0.77	14,100
Bradley	BRA13-1D	43.71348	110.75286	15.3	2.71	13,300

Belemnite and atmospheric nitrogen, respectively. LOI and TOC concentrations (LOI<sub>%</sub> and TOC<sub>%</sub>) were converted to fluxes (LOI<sub>Q</sub> and TOC<sub>Q</sub>) using bulk density values and calculated sediment accumulation rates (SAR).

Biogenic Silica was measured at continuous 2 cm intervals ( $n = 127$ ) in core JEN13-1C and processed at the University of Pittsburgh following procedures adapted from Mortlock and Froelich (1989). Wet samples were freeze-dried, homogenized to a fine powder, and treated with 30% H<sub>2</sub>O<sub>2</sub> and 1 M HCl. Biogenic silica (BSi) was extracted with 0.5 M reagent grade Na<sub>2</sub>CO<sub>3</sub> solution and determined by molybdate blue spectrophotometry at 812 nm using a Thermo Scientific Evolution 60s UV–Visible Spectrophotometer. Replicate measurements of internal sediment standards from Harding Lake, AK (Finkenbinder et al., 2014) and Twin Lakes, MT run during sample analysis yielded a precision error <0.2%. Clastic sediment concentration (Clastic<sub>%</sub>) was measured in core JEN13-1C at 2 cm intervals by calculating the residue of sediment after subtracting organic matter and biogenic silica components using: Clastic<sub>%</sub> = 100 (1 - (TOM + BSi)). Clastic<sub>%</sub> and BSi concentration (BSi<sub>%</sub>) were converted to fluxes (Clastic<sub>Q</sub> and BSi<sub>Q</sub>) using bulk density values and SAR.

### 3.2. Chronology

Age control of Teton lake sediments was established using Accelerator Mass Spectrometry radiocarbon (AMS <sup>14</sup>C) dating and tephrochronology. Samples of wood, charcoal, conifer needles, and plant macrofossils selected for AMS <sup>14</sup>C analyses were pretreated at the University of Pittsburgh using standard acid-base-acid treatments (Abbott and Stafford, 1996) and subsequently combusted, graphitized, pressed in Al targets, and measured at the W.M. Keck Carbon Cycle AMS Laboratory, University of California, Irvine. AMS <sup>14</sup>C results were calibrated and converted to calendar years before 1950 CE (cal yr BP) using CALIB v. 7.0 with the INTCAL13 calibration curve (Stuiver et al., 2005; Reimer et al., 2013). Two prominent rhyolitic tephra layers were visually observed in Teton lake cores and analyzed for major element geochemical composition at the GeoAnalytical laboratory, Washington State University, using electron probe microanalysis (EPMA). The geochemical composition of multiple size fractions from each tephra layer was compared to reference glass chemistry and combined with stratigraphic information to identify source volcano and eruption. Age-depth models for Jenny Lake cores were constructed using a smooth spline interpolation between control points and the classical age modeling (CLAM) code version 2.2 developed for the statistical software program R (Blaauw, 2010).

## 4. Results and interpretations

### 4.1. Seismic survey

Seismic profiles of Jenny Lake reveal high spatial variation in sediment distribution associated with complex lake floor

morphology (Fig. 2). Bathymetric data and seismic imagery define two primary depositional zones that comprise a broad outer shelf region and a central deep basin in front of the canyon mouth (Figs. 1 and 2). Sediment thickness is generally uniform across the broad shelf, with a consistent thickness of ~4 m blanketing a relatively flat but undulating plane. The sediment fill is greatest in the central deep basin where it reaches at least ~8 m in thickness. Prominent topographic highs in this region protrude above the lake floor and are visible in seismic profiles as acoustically opaque mounds, some partially draped with sediment. We hypothesize these features are related to the glacier and/or tectonic history of the basin (e.g. recessional moraine complexes, landslide deposits, and/or uplifted terrain associated with activity of the Teton fault). However, improved bathymetric data acquisition and further geophysical analyses are underway to securely identify these landforms.

The lowermost surface imaged by the CHIRP data is the acoustic basement (Fig. 2). We infer that the Cascade Canyon glacier was in contact with the acoustic basement during its Pinedale advance and that all sediment above this surface was deposited subsequent to the final retreat of the glacier from the lake basin during regional deglaciation (e.g. Maloney et al., 2013). Based on acoustic properties, we identify three seismic units above the acoustic basement. These are referred to as the basal unit, glacial unit, and non-glacial unit, and described briefly in chronostratigraphic order beginning with the oldest (Fig. 2). The basal unit is spatially discontinuous and more commonly observed in the central basin where it infills hollows and depressions in the basement surface. Unlike the overlying sediment packages, this unit contains irregular reflectors or is otherwise semitransparent. Its wavy upper surface and chaotic stratigraphy indicate non-uniform deposition of coarse-grained sediments and a lack of strong internal structure. The acoustic character and distribution of this unit suggest rapid deposition and we interpret it to be glacial till and/or diamict deposited in a sub-glacial or proximal proglacial setting.

Resting conformably on the basal unit or draped over the acoustic basement lies another sediment package that smoothens the uneven topography of the lower surface and is defined by a series of relatively high-amplitude reflectors that are parallel and continuous and that separate more transparent layers. The observed thickness of this unit varies from approximately 4 m in the central basin to approximately 2 m along the outer shelf. We interpret this sediment package to represent fine-grained, dense glacial lacustrine sediments that were transported by glacial meltwater. Above this lies the uppermost sediment package, which ranges in thickness from approximately 3 m in the central depocenter to approximately 1.5 m on the shelf (Fig. 2). It contains semitransparent layers separated by parallel and continuous reflectors that are generally thin and low-amplitude. The acoustic properties of this homogenous sediment unit suggest it was formed after glaciers were largely absent from the catchment. Occasional discontinuous high-amplitude reflectors in portions of this unit in the central deep basin are suggestive of discrete high-energy sedimentation events that may be related to mass movements or floods (e.g. Maloney et al., 2013).

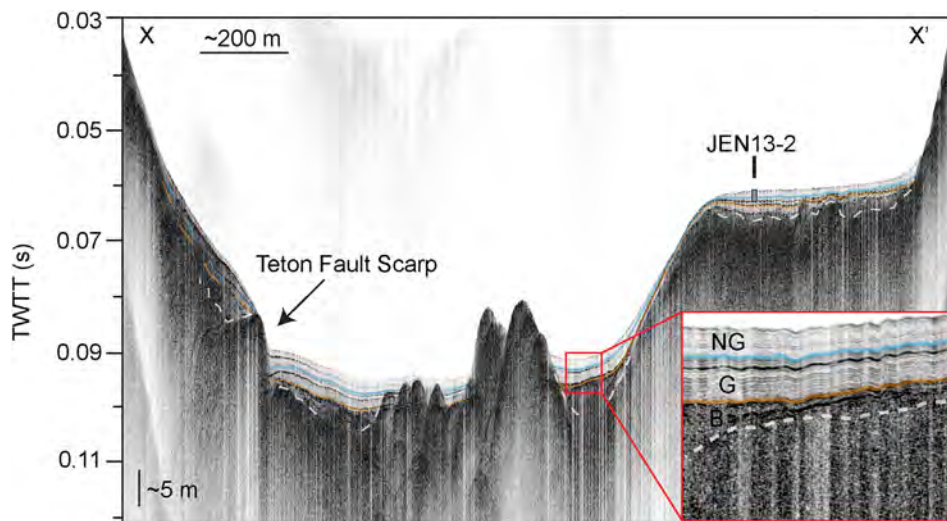


**Fig. 2.** Seismic profile (transect X-X' in Fig. 1) extending from canyon mouth across the central deep basin toward the distal eastern shore, showing lakefloor morphology, sub-bottom stratigraphy, and sediment distribution in Jenny Lake. The approximate location of core site JEN13-2 is identified along with the Teton fault scarp, which is visible on the left (western) side of profile. Inset image highlights seismic stratigraphy and primary seismic units. Colored blue and tan lines mark the bottom of the non-glacial unit (NG) and glacial unit (G), respectively. Dashed white line marks the bottom of the basal unit (B). TWT = two-way travel time (For interpretation of the references to colour in this figure legend, the reader is referred to the web version of this article.)

#### 4.2. Sediment cores

Sediment cores were collected from two sites in Jenny Lake (Fig. 1; Table 1). We focus our analyses on the longest core from

each site, JEN13-1C (256 cm-long) and JEN13-2E (209 cm-long). The lithostratigraphy of both cores is similar and consists of a two-part sequence of a relatively organic-rich olive brown homogenous unit that overlies denser light grey minerogenic silt- and clay-rich sediments (Fig. 3). The depth to the contact between the two units corresponds to a change in character of acoustic reflectors observed in seismic profiles. This transition separates the non-glacial and glacial seismostratigraphic units and we apply the same nomenclature to the two primary lithostratigraphic units identified in core section (Fig. 2). Seismic profiles reveal >2 m of glacial lacustrine sediment exists below our sediment cores.

##### 4.2.1. Geochronology

Thirteen macrofossil ages and two diagnostic tephra layers define the core age-depth models (Fig. 4; Table 2). Terrestrial plant remains suitable for radiocarbon dating are relatively abundant in the non-glacial unit and toward the top of the glacial unit. One radiocarbon sample in JEN13-1C (UCIAMS#141227) yielded an anomalously old age when compared with adjacent dates and was omitted from the age model (Fig. 4; Table 2). This sample was picked from woody plant fragments interbedded in a prominent sand horizon, which we interpret to be reworked clastic and organic material delivered from the landscape and/or littoral zone during a high-energy depositional event such as an earthquake-triggered landslide and/or seiche wave. The age of this disturbance layer in cores from both sites is ~9000 cal yr BP (Fig. 4).

Major element composition of the two tephra layers observed in the sediment sequence confirms their correlation with the Mazama (~7.6 ka; Hallett et al., 1997; Zdanowicz et al., 1999) and Glacier Peak (~13.6 ka; Kuehn et al., 2009) tephra beds (Fig. 3; Table 3). These important and widespread tephra layers have been previously noted in lake records from around the region (e.g. Whitlock, 1993). In addition to Jenny Lake, we identify the Glacier Peak tephra in a core from nearby Taggart Lake (43.70 N, 110.75 W; Fig. 1; Table 3) where it is found in non-glacial sediments, approximately 5 cm above transitional sediments and 25 cm above well-laminated silt-rich minerogenic sediments. The calibrated radiocarbon age of a macrofossil positioned ~7 cm below the tephra (i.e. near the top of

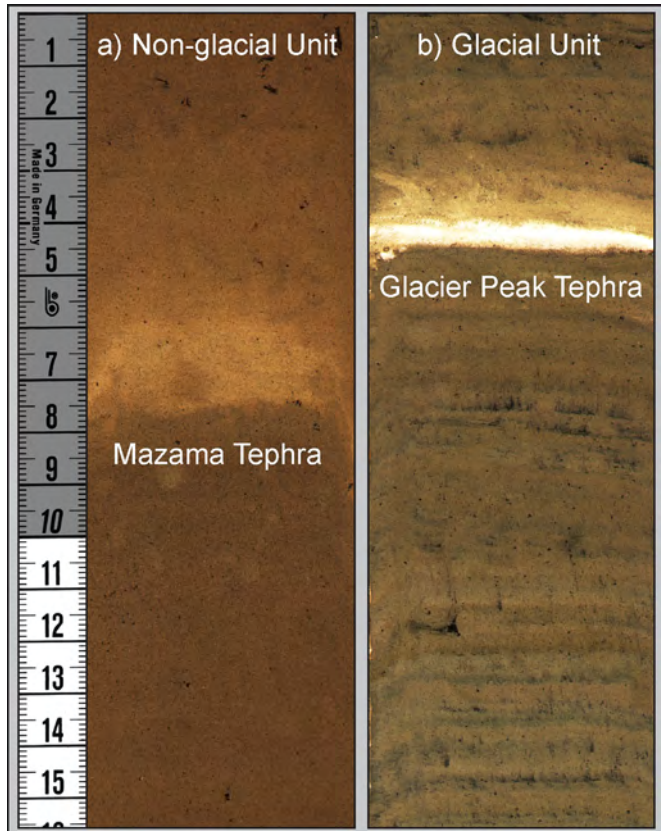


**Fig. 3.** Images of Jenny Lake sediments showing examples of (a) non-glacial and (b) glacial lithostratigraphic units. The Mazama tephra layer is visible in non-glacial panel at 7 cm depth and the Glacier Peak tephra layer is visible in glacial panel at 4 cm depth.

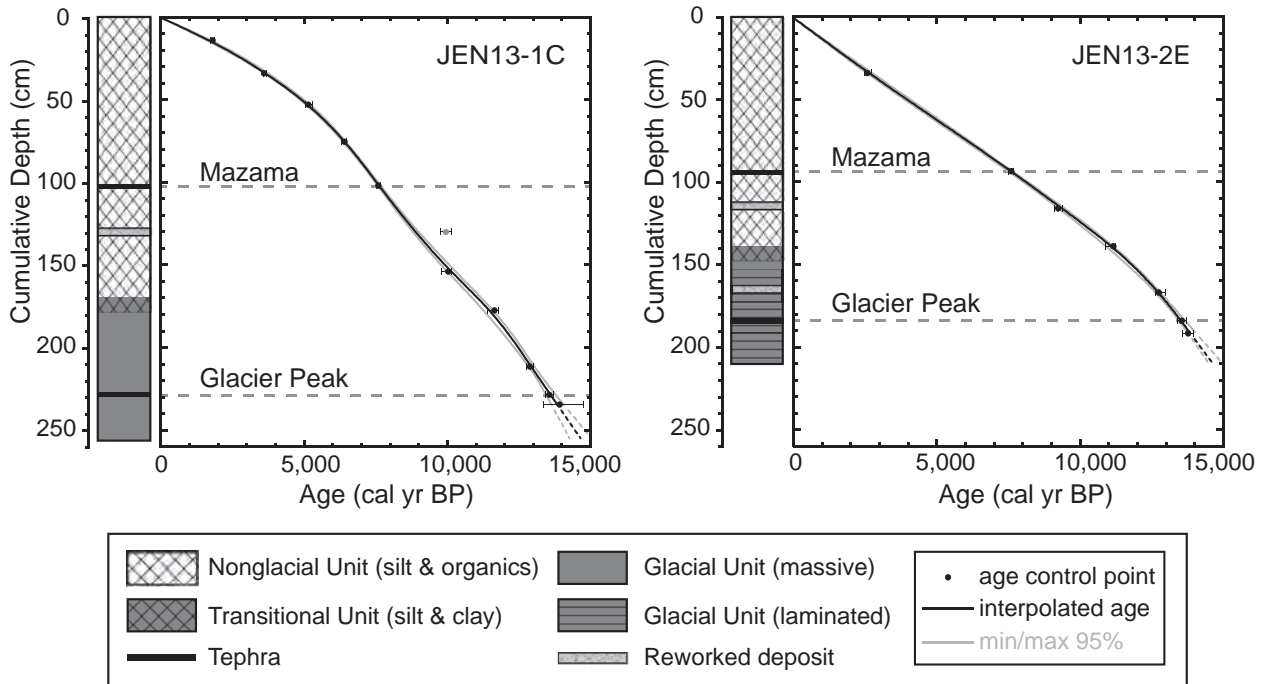


**Fig. 4.** Stratigraphy and age models for cores JEN13-1C and JEN13-2E. Core age models were generated with a smooth spline interpolation of AMS radiocarbon and tephra control points using CLAM code for R software (Blaauw, 2010). Note: one radiocarbon sample picked from a reworked disturbance deposit at 130 cm depth in JEN13-1C yielded an anomalously old age and was omitted from the age model.

**Table 2**  
Sediment core AMS radiocarbon dates and tephra ages with calibrated 2 sigma error ranges.

Sample ID (UCIAMS#)	Core	Cumulative depth (cm)	Material dated	Uncalibrated age ( <sup>14</sup> C yr BP)	Error (yr)	Calibrated age (cal yr BP) (2sigma)
141223	JEN13-1C	14.0	plant material	1865	15	1812 (1736–1866)
141224	JEN13-1C	34.0	plant material	3360	20	3603 (3563–3681)
141225	JEN13-1C	53.0	plant material	4515	20	5152 (5053–5299)
141226	JEN13-1C	75.5	wood	5630	20	6414 (6322–6467)
na	JEN13-1C	102.0	tephra	6730	40	7597 (7514–7666)
141227	JEN13-1C	130.0	wood	8845	25	9951 (9772–10,152)
141228	JEN13-1C	154.0	plant material	8865	25	10,032 (9795–10,159)
141229	JEN13-1C	177.5	charcoal	10,075	30	11,645 (11,402–11,798)
141230	JEN13-1C	211.5	charcoal	11,025	35	12,888 (12,754–13,014)
na	JEN13-1C	228.5	tephra	11,600		13,560 (13,410–13,710)
151998	JEN13-1C	234.5	plant material	12010	230	13,916 (13,367–14,764)
141220	JEN13-2E	34.0	needle	2495	20	2582 (2490–2720)
na	JEN13-2E	93.5	tephra	6730	40	7597 (7514–7666)
141221	JEN13-2E	116.0	needle	8260	35	9246 (9125–9404)
151999	JEN13-2E	139.0	plant material	9710	40	11,161 (10,881–11,227)
152000	JEN13-2E	167.0	plant material	10,850	90	12,752 (12,632–12,979)
na	JEN13-2E	184.0	tephra	11600		13,560 (13,410–13,710)
141222	JEN13-2E	191.5	plant material	11945	35	13,771 (13,580–13,979)
152001	TAG13-2A	13.0	plant material	10,880	130	12,795 (12,590–13,050)
na	TAG13-2A	34.5	tephra	11600		13,560 (13,410–13,710)
141231	TAG13-2A	42.0	wood	11,920	210	13,787 (13,283–14,417)
152002	BRA13-1D	245.0	plant material	11,425	30	13,266 (13,167–13,339)

**Table 3**  
Major element chemistry of the two tephra layers identified in Jenny Lake sediment cores. The data are normalized to 100 wt percent and the standard deviation for each major element is shown in parentheses. Results are consistent with Mazama (Hallett et al., 1997) and Glacier Peak (Kuehn et al., 2009) tephra layers.

Core ID	Depth (cm)	SiO <sub>2</sub>	Al <sub>2</sub> O <sub>3</sub>	Fe <sub>2</sub> O <sub>3</sub>	TiO <sub>2</sub>	Na <sub>2</sub> O	K <sub>2</sub> O	MgO	CaO	Cl	# shards analyzed	Tephra ID
JEN13-2E	93.5	73.11 (0.34)	14.63 (0.17)	2.1 (0.07)	0.43 (0.04)	4.76 (0.22)	2.74 (0.06)	0.46 (0.05)	1.59 (0.08)	0.18 (0.02)	17	Mazama
JEN13-2E	184.0	77.25 (0.37)	12.79 (0.17)	1.2 (0.06)	0.21 (0.04)	3.67 (0.22)	3.04 (0.15)	0.27 (0.03)	1.35 (0.07)	0.22 (0.10)	21	Glacier Peak
TAG13-2A	34.5	77.34 (0.24)	12.79 (0.14)	1.16 (0.04)	0.20 (0.02)	3.68 (0.14)	3.05 (0.13)	0.27 (0.02)	1.31 (0.07)	0.20 (0.02)	18	Glacier Peak

the transitional sediments) at Taggart Lake yields a median age of ~13,800 cal yr BP (two sigma range: 13,283–14,417 cal yr BP;

Table 2; Fig. S2). Plant material picked from non-glacial sediments near the base of a core recovered from neighboring Bradley Lake

yields an age of  $\sim 13,250$  cal yr BP (two sigma range: 13,167–13,339 cal yr BP; Table 2).

#### 4.2.2. Core stratigraphy

The glacial unit at Jenny Lake was deposited during the overall phase of up-valley recession of the Cascade Canyon glacier. This unit consists of glacial erosion products that were carried by meltwater streams and transported to the lake (e.g. Karlén, 1981; Dahl et al., 2003). While we infer that the majority of this sediment was sourced from Cascade Canyon, we acknowledge that some fine-grained sediment (e.g. fine silt and clay) delivered to Jenny Lake may have been derived from glaciers in adjacent valleys to the north. For example, during regional deglaciation, a portion of the rock flour that remained in suspension in String Lake would have been transported to Jenny Lake as glacial milk and deposited through settling in still water and/or during seasonal ice cover.

A lithostratigraphic transition between the minerogenic glacial unit and the overlying non-glacial unit captures the waning glacial influence on lake sedimentation at the termination of the Pinedale glaciation. The upper boundary of this transitional unit occurs in both Jenny Lake cores synchronously at approximately 11.0 ka (Fig. 4). The lower boundary is generally more diffuse and varies in sharpness between the two core sites, owing to differences in lithology of the glacial packages when observed in core sections. At site JEN13-1, the upper section of the glacial unit is massively bedded and gradually transitions to the non-glacial sediments above. In contrast, the glacial unit at site JEN13-2 contains cm-scale laminations and displays a slightly more abrupt upper contact (Fig. 4). We attribute these lithologic differences to the relative positions of the core sites with respect to past meltwater inflows and water depth.

Visual inspection and physical characteristics of core basal sediments suggest relatively rapid glacial lacustrine sedimentation at the start of the records. However, a lack of suitable material for radiocarbon dating precludes our ability to accurately constrain the age of the lowermost  $\sim 20$  cm sediment in both cores and age estimates for this interval necessitate a linear extrapolation of SAR from overlying sediments. Given the large potential error inherent with such an extrapolation, particularly during a period of inferred glacier recession and associated large changes in SAR, we acknowledge considerable age uncertainty during this interval and restrict our interpretations of proxy data to the dated portion of the core (past  $\sim 14$  ka) for which there is direct age control (Fig. 4). In addition, we focus our paleoenvironmental analyses on core JEN13-1C due to its more distal position (far from lake inflows) and higher sedimentary organic matter content.

#### 4.3. Physical proxies data

Physical proxies contained in core JEN13-1C display a long-term trend of decreasing values (Fig. 5). The glacial sediments are characterized by relatively high bulk density, minerogenic content, and SAR. These sediments were deposited during regional deglaciation, when substantial glacier ice occupied the watershed and the production and delivery of sediment to Jenny Lake would have been dominated by subglacial erosion and meltwater transport (e.g. Karlén, 1981). Over long timescales, both processes are dominantly controlled by glacier size, which varies according to changes in mass balance associated with the evolution of regional climate (e.g. Leonard, 1997; Larsen et al., 2012). Sediment density,  $\text{Clastic}_{\%}$ ,  $\text{Clastic}_Q$ , and SAR are all expected to decrease (increase) with decreasing (increasing) glacial erosion (e.g. Leonard, 1997; Dahl et al., 2003 and references therein). Accordingly, we interpret changes in the physical nature of Jenny Lake sediment during the glacial unit to track the pattern of glacier recession in Cascade Canyon in response to climate changes occurring at the end of the last ice age.

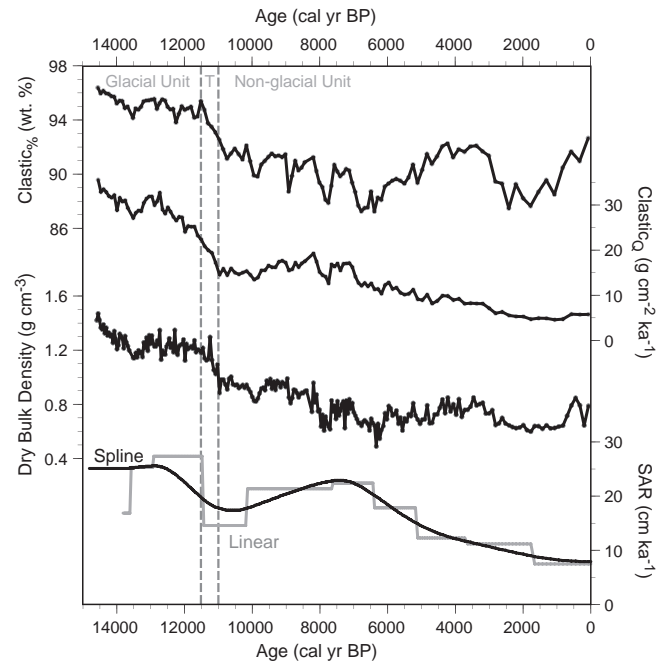


Fig. 5. Physical parameters of Jenny Lake sediments measured in core JEN13-1C, including clastic sediment concentration ( $\text{Clastic}_{\%}$ ) and flux ( $\text{Clastic}_Q$ ), sediment bulk density, and sediment accumulation rates (SAR). The glacial and non-glacial lithostratigraphic units are shown separated by a thin transitional unit (T) from  $\sim 11.5$  ka to  $\sim 11.0$  ka. Unit boundaries (dashed vertical grey lines) were determined based on shifts in sediment character and proxy data observed in cores from sites JEN13-1 and JEN13-2 and corroborated by seismic stratigraphy. Note: SAR is shown calculated using both a smooth spline and linear interpolation of age control points.

$\text{Clastic}_{\%}$  and  $\text{Clastic}_Q$  decline from maximum values (96% and  $35 \text{ g cm}^{-2} \text{ ka}^{-1}$ , respectively) at the core bottom, but maintain generally high and constant values until  $\sim 11.5$  ka (Fig. 5). Changes in clastic sediment delivery to alpine lakes can indicate long-term variations in erosion rates and shorter-term disturbance events such as fires, floods, earthquakes, and landslides. However, in glacier occupied catchments, clastic sediment flux is dominantly controlled by changes in glacier extent (e.g. Abbott et al., 1997; Rodbell et al., 2008). The early trend in clastic sediment parameters at Jenny Lake reflects continued glacier recession leading up to the start of the record followed by an interval of persistent small glacier activity during the final phase of deglaciation.

The lithologic transition from glacially influenced sedimentation to non-glacial sedimentation is recorded as a pronounced decrease in all four physical proxies between  $\sim 11.5$  ka and  $\sim 11.0$  ka (Fig. 5). Following this shift,  $\text{Clastic}_Q$  and SAR remain stable and increase modestly until  $\sim 7.5$  ka before gradually decreasing through the mid and late Holocene toward modern minimum values of  $5 \text{ g cm}^{-2} \text{ ka}^{-1}$  and  $8 \text{ cm ka}^{-1}$ , respectively (Fig. 5). Sediment bulk density and  $\text{Clastic}_{\%}$  are strongly correlated throughout the record ( $R^2 = 0.89$ ,  $n = 124$ ). Both proxies reach minimum values around 6.5 ka (Fig. 5).  $\text{Clastic}_{\%}$  increases markedly from 6.0 ka to 3.5 ka before decreasing to a broad local minimum  $\sim 2.0$  ka and increasing through the past eight centuries, reaching relatively high values in modern time (Fig. 5).

#### 4.4. Biological and geochemical proxies data

Organic matter (OM) and geochemical parameters contained in Jenny Lake sediments show substantial changes between the glacial and non-glacial units (Fig. 6). Lake sedimentary OM is derived from a combination of terrestrial and aquatic sources that

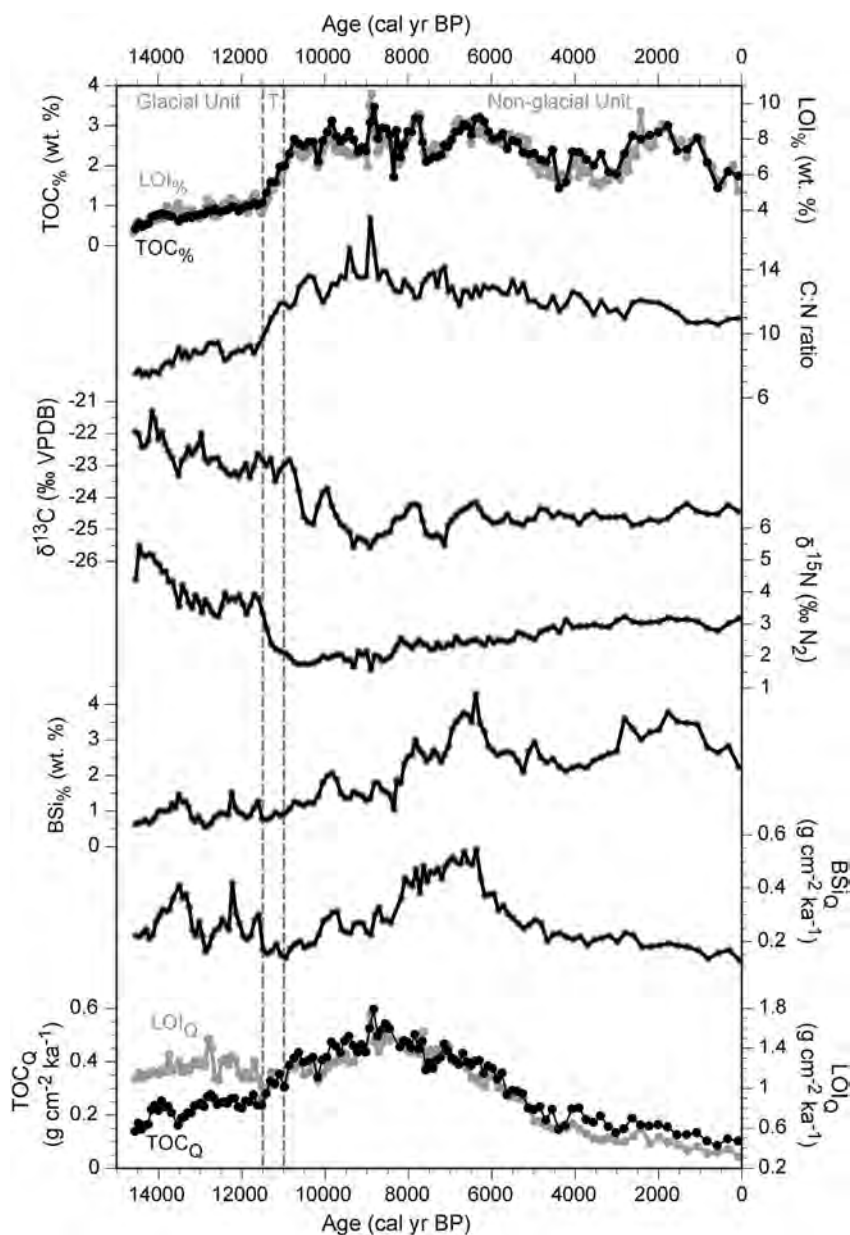


**Fig. 6.** Total organic carbon (TOC%), loss on ignition (LOI%), organic matter C:N, stable carbon and nitrogen isotopes ( $\delta^{13}\text{C}$  and  $\delta^{15}\text{N}$ ), biogenic silica weight percent (BSi%) and flux (BSi<sub>Q</sub>), and the mass flux of total organic carbon (TOC<sub>Q</sub>) and total organic matter (LOI<sub>Q</sub>), from core JEN13-1C. Dashed vertical grey lines mark the boundaries between glacial, transitional (T), and non-glacial lithostratigraphic units.

can be distinguished by their characteristic elemental and isotopic signatures. The elemental carbon and nitrogen mass ratio (C:N) of lake algae is typically between 4 and 10, while soils and vascular plants have values  $> 10$  (Meyers and Teranes, 2001; Larsen et al., 2011). Additionally, variations in the carbon isotopic composition ( $\delta^{13}\text{C}$ ) of sedimentary OM in oligotrophic lakes can dominantly reflect the relative contribution of OM sources, rather than changes in primary productivity or nutrient availability (e.g. Langdon et al., 2010). At Jenny Lake, the similarity of these proxies is evidenced by the strong correlation of C:N with  $\delta^{13}\text{C}$  ( $R^2 = 0.79$ ,  $n = 127$ ; Fig. 7a) and coupled changes in both parameters are used to infer variations in OM source. Values of C:N and  $\delta^{13}\text{C}$  range from  $\sim 7$  to  $\sim 17$  and  $25.5\text{‰}$  to  $21.3\text{‰}$ , respectively (Fig. 6), and indicate an algal OM source prior to 11.5 ka and a mixed algal-terrestrial source thereafter (Fig. 7a). Maximum C:N and minimum  $\delta^{13}\text{C}$  values occur synchronously at  $\sim 9.0$  ka and are associated with one sample

picked from the disturbance deposit identified in core section (Fig. 4). Due to the high concentration of woody terrestrial plant material observed in this deposit, we interpret these values to represent an approximate terrestrial end member of sedimentary OM and use them as a reference for evaluating changes in OM source contribution to Jenny Lake sediments.

LOI% values range from  $\sim 4\%$  to  $\sim 10\%$  and show a strong correlation to TOC% ( $R^2 = 0.93$ ,  $n = 124$ ; Fig. 6). Average TOC% (and LOI%) values are  $0.7 \pm 0.2\%$  ( $3.9 \pm 0.4\%$ ) during the glacial unit and  $2.4 \pm 0.5\%$  ( $7.4 \pm 1.0\%$ ) during the non-glacial unit. Low TOC% during the glacial unit is associated with low C:N, more positive  $\delta^{13}\text{C}$  values, and high Clastic% (Fig. 7). The onset of increased organic matter accumulation occurs  $\sim 11.5$  ka and sustained elevated values are reached by 10.8 ka. This increase coincides with a shift toward higher C:N values and more negative  $\delta^{13}\text{C}$  (Figs. 6 and 7a). High average organic matter concentration persists from 10.8 ka to 6.0 ka, with a notable

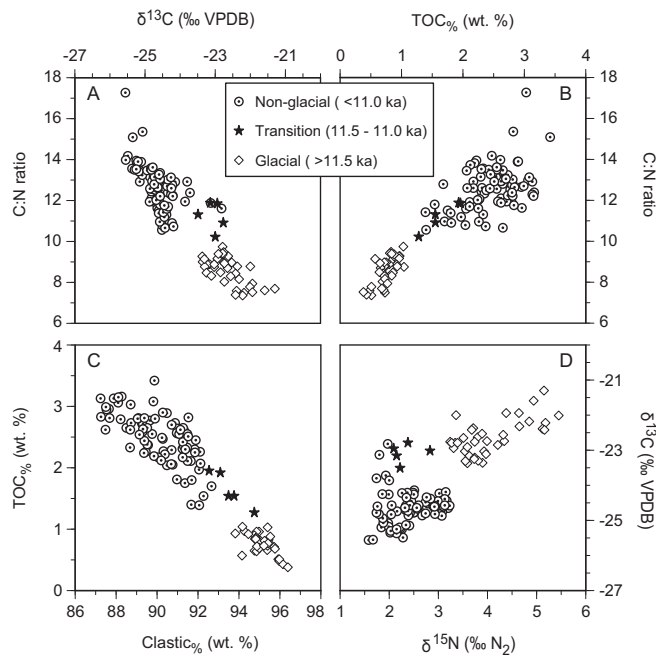


**Fig. 7.** Cross-plots of Jenny Lake sediment data highlighting relationships between: A) organic matter C:N and stable carbon isotopes ( $\delta^{13}\text{C}$ ); B) organic matter C:N and total organic carbon ( $\text{TOC}_x$ ); C) total organic carbon ( $\text{TOC}_x$ ) and clastic sediment concentration ( $\text{Clastic}_x$ ); and D) organic matter stable carbon and nitrogen isotopes ( $\delta^{13}\text{C}$  and  $\delta^{15}\text{N}$ ). Distinct relationships between sediment physical and geochemical parameters were used in conjunction with observed changes in sediment lithology to differentiate between the glacial, transitional, and non-glacial lithostratigraphic units discussed in the text.

decrease between 7.7 ka and 7.0 ka. From 6.0 ka to present,  $\delta^{13}\text{C}$  remains stable at  $-24.5\text{‰}$  and C:N is stable, but gradually decreasing (Fig. 6). Organic matter concentration is generally anti-correlated with  $\text{Clastic}_x$  ( $r^2 = 0.94$ ;  $n = 124$ ; Fig. 7c) and shows intervals of decreased values from 6.0 ka to 2.8 ka and during the past millennium that are separated by a local peak in the late Holocene. The  $\text{TN}_x$  values (not shown) are relatively low during the glacial unit and generally higher but variable during the non-glacial unit, with a trend that correlates well with  $\text{TOC}_x$  ( $R^2 = 0.95$ ,  $n = 127$ ). Sedimentary  $\delta^{15}\text{N}$  varies from  $-1.5\text{‰}$  to  $-5.5\text{‰}$ . Variations in the  $\delta^{15}\text{N}$  of sedimentary OM can reflect changes in productivity, diagenetic processes, and/or the relative sources and isotopic composition of nitrogen supplied to lakes (Meyers and Teranes, 2001; Talbot, 2001). The  $\delta^{15}\text{N}$  values are high throughout the glacial unit and decrease sharply beginning  $\sim 11.5$  ka in accordance with the transition to non-glacial sedimentation (Figs. 6 and 7d). Minimum  $\delta^{15}\text{N}$  values ( $<2\text{‰}$ ) occur between  $\sim 10.8$  ka and  $\sim 8.5$  ka, and are followed by steadily increasing values during the middle and late Holocene.

Biogenic silica, a proxy for diatom abundance, ranges from  $\sim 1\%$  to  $4\%$  and displays a broad trend of increasing values throughout the record, reaching two broad maxima at  $\sim 6.5$  ka and  $\sim 2.0$  ka (Fig. 6). Changes in  $\text{BSi}_x$  may be influenced by changes in sedimentation rate in addition to changes in primary productivity. We convert  $\text{BSi}_x$  to  $\text{BSi}_Q$  in an attempt to evaluate changes in primary productivity independent of changes in minerogenic and organic matter input.  $\text{BSi}_Q$  is variable at the start of the record and increases gradually through the transition to non-glacial conditions (Fig. 6). A broad peak in  $\text{BSi}_Q$  from 9.0 ka to  $\sim 6.5$  ka is followed by a decrease and subsequent trend of low and stable values that persist through the late Holocene.

## 5. Discussion

### 5.1. Deglaciation and postglacial environmental conditions in the Teton Range

Jenny Lake seismic stratigraphy and sediment core proxy data provide a record of deglaciation and postglacial environmental conditions in the Teton Range. The prominent two-part lithostratigraphic sequence observed in the sediment cores is evinced through cross-plots of proxy data (Fig. 7). Distinct relationships between physical, biological, and geochemical parameters highlight characteristic differences between the glacial and non-glacial units, which are separated by a brief transitional unit between  $\sim 11.5$  ka and  $\sim 11.0$  ka. These relationships guide our interpretations of individual proxies during respective periods of glacial and non-glacial depositional environments at Jenny Lake and provide a framework for evaluating changes in glacier extent and environmental conditions in the Tetons. In the following discussion, we present the lake sediment record in the context of latest Pleistocene and Holocene climate variability in the northern Rockies, placing an emphasis on the pattern of glacier recession and periods of notable postglacial environmental changes, and on comparisons to regional paleoclimate datasets.

#### 5.1.1. Deglacial chronology

The start of continuous sediment accumulation at Jenny Lake marks the timing of initial irreversible retreat of the Cascade Canyon glacier. It is not possible to place absolute constraints on the timing of deglaciation because the cores do not extend to the base of the glacial unit. Instead, we use available core data to provide a minimum limiting age for lake inception and to qualitatively track the glacier's subsequent up-valley progression.

Lowermost radiocarbon dates from Jenny Lake cores at sites JEN13-1 and JEN13-2 are  $\sim 13,900 \pm 700$  cal yr BP and  $\sim 13,800 \pm 200$  cal yr BP, respectively (Table 2). These ages indicate that much of the glacial unit identified in the seismic stratigraphy, which extends below the base of the cores, was deposited prior to 13.8 ka. Based on radiocarbon dates, core lithology, core SAR, and seismostratigraphy, we infer that Jenny Lake sediment accumulation began centuries before 13.8 ka, and that by this time the glacier had retreated a substantial distance up-valley in response to climate driven changes in glacier mass balance.

Additional support for reduced glacier extent by 13.8 ka comes from nearby Bradley and Taggart Lakes (Fig. 1). The non-glacial character of Bradley Lake sediment at  $\sim 13.3$  ka indicates that the glacier occupying Garnet Canyon had either completely melted or was greatly reduced and contributing minimal sediment to the lake. This implies that deglaciation of Garnet Canyon initiated many centuries prior to 13.3 ka. At Taggart Lake, a relatively rapid switch from transitional sediments to organic-rich non-glacial sediments occurs immediately after  $\sim 13.8$  ka but before the deposition of the Glacier Peak tephra ( $\sim 13.6$  ka; Kuehn et al., 2009), which is found in overlying non-glacial sediment (Table 2; Fig. S2). An earlier change in sediment character from well-laminated glacial sediments to transitional sediments marks a substantial reduction in the delivery of glacier erosion products to Taggart lake and likely corresponds to the formation of an upstream sediment trap at either Lake Taminah or Snowdrift Lake as the Avalanche Canyon glacier retreated past one of these up-valley basins (e.g. Karlén, 1981; Dahl et al., 2003). Lake Taminah, situated at an elevation of  $\sim 2800$  m asl, is the lower of the two lakes, located approximately 65% (4.5 km) of the way up the main fork of Avalanche Canyon from the inner moraine impounding Taggart Lake (Fig. 1). The position of this basin provides a conservative constraint on the amount of ice retreat in Avalanche Canyon accomplished by the start of the Jenny Lake

sediment core record. We acknowledge that glaciers in adjacent valleys likely had different response times because of differences in their catchment characteristics (e.g. drainage area, slope, aspect, hypsometry) and that the inferred near-disappearance of the Garnet Canyon glacier and a minimum retreat of 65% for the Avalanche Canyon glacier cannot be directly correlated to the position of the Cascade Canyon glacier. Nonetheless, we use this information to provide a context for the relative position of the Cascade Canyon glacier at the start of the record and to posit that glacier extents in the Tetons were greatly reduced by 13.8 ka.

Decreasing sediment density, Clastic%, and Clastic<sub>Q</sub> in JEN13-1 from the core base to ~13.5 ka indicates generally continuous glacier recession (Fig. 5). A subsequent interval of high Clastic<sub>Q</sub> and a plateau in sediment density persists until ~11.5 ka and coincides with uppermost glacial sediments identified in core lithology (Fig. 5). We interpret sediment physical characteristics during this interval to reflect a sustained period of lingering glacier erosion or landscape instability in the catchment. Today, small remnant glaciers and ice fields exist in scalloped northerly aspects (e.g. north-facing cirques) at higher elevations and areas fed by high snow accumulation in the upper reaches of Cascade Canyon. These features are considered vestiges of the Little Ice Age (LIA; ~1250–1900 CE), the most recent Neoglacial period of widespread alpine glacier expansion (Denton and Karlén, 1973; Davis, 1988). Moraine complexes from extant cirque glaciers in the Tetons reflect glacier advances during the LIA (e.g. Fryxell, 1935; Mahaney, 1975) and evidence for earlier periods of Neoglacial expansion have been identified on select moraines (e.g. Mahaney, 1975; Mahaney and Spence, 1984). Our core data indicate that Neoglacial ice growth in Cascade Canyon did not result in distinct glacial sedimentation at Jenny Lake. Despite inferred differences in landscape stability (and thus potential sediment yield) between the late Pleistocene and late Holocene, we suggest that the glacial character of Jenny Lake sediment between ~13.5 and 11.5 ka reflects small glacier advances in Cascade Canyon and that cirque glacier extents during this interval exceeded those achieved during Neoglaciation.

A shift in all physical and geochemical proxies at 11.5 ka marks the onset of non-glacial sedimentation at Jenny Lake. The step-like drop in density and Clastic<sub>Q</sub> indicates reduced erosion and transport of minerogenic material to the lake, suggesting that cirque glaciers had disappeared or were no longer contributing appreciably to lake sedimentation (Fig. 5). Although it is possible that small cirque glaciers were maintained after this time (for example positioned in basins upstream of sediment traps, in topographically shaded locations, or areas with enhanced accumulation), we place the end of deglaciation at 11.5 ka when Jenny Lake proxies indicate the termination of glacial lacustrine sedimentation.

### 5.1.2. Postglacial environments

The pattern of deglaciation outlined above provides the chronological framework for environmental changes recorded at Jenny Lake. Glacier recession reflects progressively warmer summer temperatures and drier conditions in the Tetons during the latest Pleistocene. Despite the high influx of clastic material and inferred turbid water column during the glacial unit, elevated LOI<sub>Q</sub> values indicate relatively high sedimentary organic matter accumulation. More positive  $\delta^{13}\text{C}$ , low C:N, variable BSi<sub>Q</sub>, and high LOI<sub>Q</sub> relative to TOC<sub>Q</sub>, suggest organic matter production was dominated by aquatic plants and algae. Increased primary productivity in Jenny Lake during deglaciation is consistent with modern alpine lake systems in the Rocky Mountains where average primary productivity rates are up to five times higher in glacier-fed lakes than their non-glacial (snowmelt-fed) counterparts (Slemmons and Saros, 2012). Productivity in glacier-fed lakes is linked to higher levels of dissolved inorganic nitrogen (i.e. nitrate) in glacial meltwater, but

interestingly the source and underlying cause for elevated nitrogen levels are not well defined (e.g. Williams et al., 2007; Baron et al., 2009; Saros et al., 2010). At Jenny Lake, high  $\delta^{15}\text{N}$  values during the glacial unit point toward a source pool of isotopically enriched N that was produced on, in, or below the glacier and/or inorganically bound to clay-rich glacier erosion products delivered to the lake (Talbot, 2001). Additional explanations for high  $\delta^{15}\text{N}$  values at this time could be related to isotopic enrichment of dissolved N in lake water due to physiological fractionation under N-limiting conditions and/or diagenetic processes (e.g. Talbot, 2001). However, inferred lake conditions (e.g. highly-oligotrophic, well-mixed, high SAR) suggest these effects would have been secondary or negligible. The coherent pattern of high  $\delta^{15}\text{N}$  values during the glacial unit and subsequent sharp transition to lower values that is coincident with the transition to non-glacial conditions indicates a relationship between glacier meltwater and  $\delta^{15}\text{N}$  values (Fig. 6). We highlight this relationship to suggest that in similar lake systems,  $\delta^{15}\text{N}$  may be an indicator of glacier meltwater and serve as a useful complementary proxy for glacier reconstructions derived from lake sediments.

The transition from glacial to non-glacial conditions at the start of the Holocene is the most notable feature in paleolimnologic development of Jenny Lake. Prior to ~11.5 ka, glacier processes dominated lake sedimentation and organic matter proxies suggest little soil development or vegetation in the catchment (Figs. 6 and 7). The subsequent shift to higher OM accumulation with high C:N values and low  $\delta^{13}\text{C}$  values reflects soil development and colonization of the freshly deglaciated landscape by vegetation, while decreases in Clastic<sub>Q</sub> and SAR reflect catchment stabilization under non-glacial conditions (Figs. 5 and 6).

The early Holocene is characterized by high and increasing organic matter concentration and flux. Maximum BSi<sub>Q</sub> from ~8.0 to ~6.5 ka overlaps a broad peak in TOC<sub>Q</sub> from ~10.0 ka to ~6.5 ka, and together define a period of inferred mild conditions with higher productivity (Fig. 6). TOC<sub>Q</sub> and BSi<sub>Q</sub> decrease after 6.0 ka, and TOC<sub>Q</sub> maintains a steady decline toward present, suggesting a gradual shift toward cooler conditions in the catchment and/or increasing catchment stability. Reduced erosion and increased landscape stabilization during the past 6 ka are indicated by long-term decreases in both Clastic<sub>Q</sub> and SAR (Fig. 5). This long-term trend may reflect reduced fluvial erosion in Cascade Canyon and/or increased landscape stability associated with increased vegetation cover and more stable geomorphic conditions on valley hillslopes.

## 5.2. Comparison to regional and relevant climate records

### 5.2.1. Deglaciation

The timing and pattern of deglaciation presented here adds to an extensive body of work devoted to unraveling the history of Pinedale-age glacier fluctuations in the collective Yellowstone, Teton, and Wind River region (e.g. Pierce et al., 1976, 2011; Pierce, 1979; Colman and Pierce, 1981; Zielinski and Davis, 1987; Davis, 1988; Davis et al., 1998; Love et al., 1992, 2003; Whitlock, 1993; Gosse et al., 1995a, 1995b; Phillips et al., 1997; Licciardi et al., 2001; Sharp et al., 2003; Licciardi and Pierce, 2008). Moraine chronologies suggest retreat of Teton alpine glaciers from their Pinedale termini was substantially delayed relative to most western U.S. glaciers (e.g. Licciardi and Pierce, 2008; Young et al., 2011), potentially related to altered westerly atmospheric flow and moisture delivery to the Tetons (e.g. Licciardi and Pierce, 2008). Sediment from Jenny, Bradley, and Taggart Lakes indicate that glacier extents in the Tetons were greatly reduced by 13.8 ka. This age (and the inferred earlier dates for lake inception) suggests that the timing of glacier retreat in Teton valleys is coincident with the Bølling-Allerød warm period recorded in Greenland ice cores

(Fig. 8; Rasmussen et al., 2006; Vinther et al., 2006). The Bølling-Allerød, which began ~14.7 ka, represents the first period of sustained warming in the Northern Hemisphere following the Last Glacial Maximum. The near synchronous retreat of western U.S. alpine glaciers (e.g. Licciardi et al., 2004; Young et al., 2011) implies a coordinated response to a common driver and it has been suggested that widespread ice retreat may have been driven by this warming event (Young et al., 2011). Evidence for warming conditions in the Tetons during this time comes from fossil pollen assemblages in Hedrick Pond, a small lake ~10 km east of Jenny Lake, which reveal a trend of increasing *Pinus* taxa and Parkland vegetation (Whitlock, 1993, Fig. 8).

The inferred onset date and relatively rapid style of ice retreat derived from lake sediments apparently contrasts with a transect of three  $^{10}\text{Be}$  exposure ages obtained from polished bedrock in Garnet Canyon, which suggest ice retreat in this canyon was delayed until approximately 12 ka ( $12 \pm 2$  ka) and occurred gradually (Tranel et al., 2015). Lake sediment ages compare more favorably with a  $^{10}\text{Be}$  exposure age chronology for Cascade Canyon (Licciardi and

Pierce, 2008). Excluding two outliers attributed to prior exposure, eight boulders resting on the terminal moraine complex impounding Jenny Lake yield a mean  $^{10}\text{Be}$  exposure age of  $15.1 \pm 1.2$  ka (Fig. 8; mean exposure age and uncertainty recalculated from Licciardi and Pierce (2008) using the CRONUScal (Marrero et al., 2016) with LSDn scaling (Lifton et al., 2014) and provided by J.M. Licciardi, written comm., 2016). We hypothesize that potential discrepancies between exposure ages and lake sediment ages may be related to geological and analytical uncertainties inherent to  $^{10}\text{Be}$  exposure age dating, particularly those associated with the nuclide production rates and scaling (e.g. Licciardi and Pierce, 2008). Ideally, basal ages from sediment cores that penetrate ice-proximal deposits, combined with additional exposure ages of glacial landforms in corresponding catchments, will be used to test this hypothesis. We suggest that future paired sediment core and landform exposure ages from the Tetons can be used to minimize geological uncertainties and/or refine local exposure age calculations. Improved glacier chronologies from multiple adjacent canyons may then also be used to further test hypotheses regarding

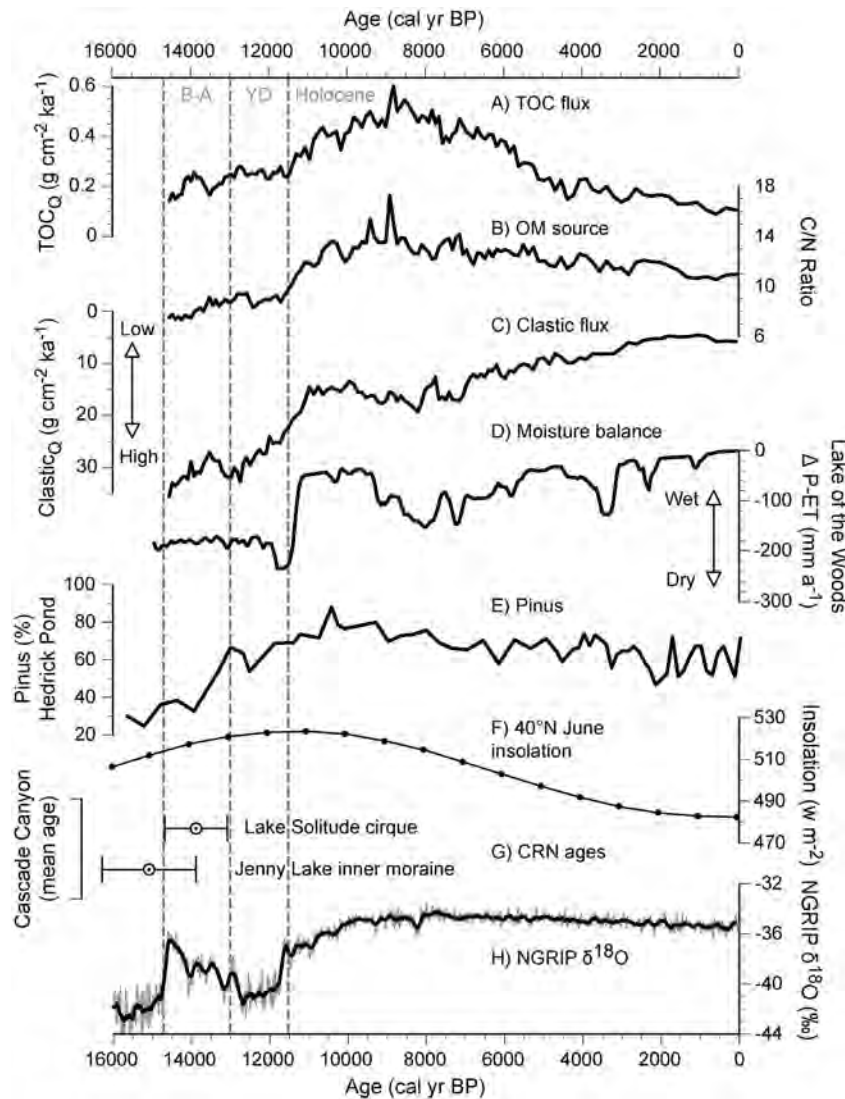


**Fig. 8.** Comparison of Jenny Lake  $\text{TOC}_Q$ , C:N, and  $\text{Clastic}_Q$  (A–C), with select regional and relevant climate records: (D) effective moisture balance reconstructed at Lake of the Woods, WY (Pribyl and Shuman, 2014); (E) *Pinus* pollen concentration from Hedrick Pond, WY (Whitlock, 1993); (F) 40°N June insolation (Berger and Loutre, 1991); (G) Mean  $^{10}\text{Be}$  exposure ages of boulders in Cascade Canyon recalculated from Licciardi and Pierce (2008) using the CRONUScal (Marrero et al., 2016) with LSDn scaling (Lifton et al., 2014); (H) Greenland ice core  $\delta^{18}\text{O}$  values (North Greenland Ice Core Project members, 2004). Dashed vertical grey lines mark boundaries between recognized intervals of climate change in the Northern Hemisphere (B–A = Bølling-Allerød, YD = Younger Dryas).

climatic and non-climatic (e.g. geologic) controls on alpine glacier response times and the apparent delayed onset of deglaciation in the Tetons relative to nearby ranges (e.g. Licciardi et al., 2004; Thackray et al., 2004; Licciardi and Pierce, 2008; Thackray, 2008; Foster et al., 2010; Young et al., 2011 and references therein).

### 5.2.2. Younger Dryas period

Lingering glacier activity in Cascade Canyon between 13.5 and 11.5 ka coincides with Younger Dryas cooling. The Younger Dryas is characterized in Greenland ice cores as a major cooling event and return to glacial conditions that punctuated Bølling-Allerød warming (Fig. 8). Modest cirque glacier advances during the Younger Dryas have been identified in the Wind River Range, WY (Zielinski and Davis, 1987; Gosse et al., 1995a, 1995b), the Lewis Range, MT (Schachtman et al., 2015), the Front Range, CO (Menounos and Reasoner, 1997), and other mountain ranges in the western U.S. (e.g. Licciardi et al., 2004 and references therein). Our sedimentary evidence for cirque glacier growth in Cascade Canyon at this time apparently predates a mean exposure age of  $13.9 \pm 0.7$  ka for the Lake Solitude cirque (~90% of the way up Cascade Canyon), derived from 3 boulders resting on the cirque lip and previously associated with a Younger Dryas advance (mean exposure age and uncertainty recalculated from Licciardi and Pierce (2008) using the CRONUScalc (Marrero et al., 2016) with LSDn scaling (Lifton et al., 2014) and provided by J.M. Licciardi, *written comm.*, 2016). In addition, pollen reconstructions from lake sites in the region reveal vegetation shifts interpreted to indicate cooler temperatures (Whitlock, 1993; Reasoner and Jodry, 2000). Despite the combined evidence for cooling and small glacier advances during this period, there remains debate over the impact of the Younger Dryas event and the response of alpine glaciers in North America (e.g. Young et al., 2012). Here, we demonstrate that active glaciers were present in the Tetons during the Younger Dryas and were likely larger than at any time in the past 11.5 ka, including during the LIA.

### 5.2.3. Onset of non-glacial conditions and Holocene environmental changes

The transition to non-glacial conditions at Jenny Lake after 11.5 ka likely reflects a shift toward warmer summers and increased landscape stability in the Tetons. This event coincides with maximum Northern Hemisphere summer insolation and a shift to higher temperatures over Greenland (Fig. 8). Regionally, this transition is also accompanied by a major increase in effective moisture and wetter conditions in the nearby Wind Rivers (Shuman et al., 2010; Pribyl and Shuman, 2014) and occurs at a time when pollen assemblages at Hedrick Pond reflect well-developed parkland forests (Whitlock, 1993, Fig. 8). Lacustrine evidence for upslope tree-line migration in Wyoming and Idaho imply a shift to warmer summers at the onset of the Holocene (Brunelle and Whitlock, 2003; Mensing et al., 2012). In Glacier National Park, sediments in Swiftcurrent Lake indicate warmer summers and the retreat of the Grinnell Glacier ~11.5 ka, following the termination of its Younger Dryas advance (Schachtman et al., 2015). Multiple lakes in northern Yellowstone record wetter conditions in the early Holocene (e.g. Whitlock et al., 2012 and references therein), but spatial heterogeneity is evident (e.g. Krause et al., 2015). The apparent lag of Jenny Lake proxy data behind forest succession at Hedrick Pond and other proximal low elevation lakes may reflect the delayed timing of alpine glacier recession in high elevation Teton catchments relative to ice retreat of the southern margin of the Yellowstone Ice Cap (Whitlock, 1993; Licciardi and Pierce, 2008, Fig. 8).

We infer warmer conditions at Jenny Lake between ~10.0 ka and 6.5 ka when many sites in the Rocky Mountains register drier conditions (Shuman et al., 2009, 2010 and references therein) and

or warmer summer temperatures than present (Mensing et al., 2012; Mumma et al., 2012 and references therein). Long-term decreases in the flux of organic matter and clastic material to Jenny Lake during the past 6 ka are paced by the monotonic decline in summer insolation and inferred cooling (Fig. 8). Increasing landscape stability through this time is consistent with generally wetter conditions in the Wind Rivers, which may have promoted greater vegetation cover and hillslope stabilization (Fig. 8). Relative changes in sediment composition (i.e.  $\text{Clastic}_{\%}$ ,  $\text{LOI}_{\%}$ ,  $\text{BSi}_{\%}$ ) during the past 4 ka reflect substantial changes in lake productivity and/or surface processes in the catchment (e.g. sediment production and transport) and hint at substantial late Holocene climate variability. However, these changes are muted by the overall low sediment accumulation rate and inferred oligotrophic character of the lake through this time. The comparatively stable character of the proxy data during the Holocene relative to the latest Pleistocene may reflect differences in landscape stability in the Tetons and the sensitivity of the Jenny Lake system to environmental and landscape changes during glacial and non-glacial conditions.

## 6. Conclusions

Sediments in Jenny Lake record the timing and pattern of deglaciation and preserve a continuous and datable record of postglacial environmental changes in the Teton Range. Seismic reflection profiles demonstrate high spatial variability in sediment distribution within the lake and reveal landforms associated with a dynamic history of glacier fluctuations. The principle seismostratigraphic units correspond to an interval of dense, minerogenic glacial lacustrine sedimentation followed by an interval of non-glacial sedimentation. This two-part sequence is observed in the lithostratigraphy of multiple sediment cores recovered from Jenny Lake and other nearby lakes, revealing a postglacial pattern of sedimentary succession that is consistent within individual basins and between lakes from adjacent valleys.

Core data and seismic stratigraphy suggest deglaciation of alpine glaciers in the Tetons initiated centuries prior to 13.8 ka, and demonstrate that by this time glacier extents were greatly reduced. Core proxy data also suggest that continuous rapid ice recession in Cascade Canyon was underway by 14 ka but was slowed by an interval of small glacier activity ~13.5 ka to ~11.5 ka. The end of glacial lacustrine sedimentation ~11.5 ka marks the transition to non-glacial conditions at Jenny Lake and multiple physical and organic matter proxies reflect a shift toward warmer summers with increased vegetation cover and landscape stability in the Tetons. Environmental parameters indicate generally stable Holocene conditions in Cascade Canyon. A period of inferred mild conditions with higher primary productivity and vegetation cover persisted until ~6.5 ka. The transition out of inferred mild conditions during the middle Holocene is paced by the gradual decline in summer insolation and coincide with generally wetter conditions in the region. Long-term reductions in soil erosion and lake productivity reflect increased catchment stability and cooler conditions, respectively, and compose a trend that persists through the late Holocene and to present day.

## Acknowledgements

We thank Whitney Doss, Diana Larsen, Kate Elkind, Sarah Crump, Lance Larsen, Sarah Spaulding, Marc Serravezza, and the LacCore staff for field and/or laboratory assistance. We also thank: Devin Hougardy for help performing the seismic survey and acquiring CHIRP data; National Park Service (NPS) personnel Kathy Mellander, Sue Consolo-Murphy, and Scott Guenther for logistical support; Gifford Miller and the Wyoming Game and Fish

Department for providing field equipment; Joe Licciardi for providing updated exposure ages; and Keck Carbon Cycle AMS Lab personnel John Southon, Guaciarra dos Santos, and Chanda Bertrand, for assistance with radiocarbon samples. This work was funded in part by a NPS Grand Teton Association Boyd Evison fellowship, an Explorers Club Eddie Bauer youth grant, a joint University of Wyoming–NPS Research Center grant, and funds from the University of Pittsburgh. Finkenbinder acknowledges support from a University of Pittsburgh Mellon Predoctoral Fellowship. We thank Kenneth L. Pierce and an anonymous reviewer for improving this manuscript through external reviews.

## Appendix A. Supplementary data

Supplementary data related to this article can be found at <http://dx.doi.org/10.1016/j.quascirev.2016.02.024>.

## References

- Abbott, M.B., Stafford, T.W., 1996. Radiocarbon geochemistry of modern and ancient Arctic lake systems, Baffin Island, Canada. *Quat. Res.* 45, 300–311.
- Abbott, M.B., Seltzer, G.O., Kelts, K.R., Southon, J., 1997. Holocene paleohydrology of the tropical Andes from Lake records. *Quat. Res.* 47, 70–80.
- Arendt, A.A., Echelmeyer, K.A., Harrison, W.D., Lingle, C.S., Valentine, V.B., 2002. Rapid wastage of Alaska glaciers and their contribution to rising sea level. *Science* 297, 382–386.
- Baron, J.S., Schmidt, T.M., Hartman, M.D., 2009. Climate-induced changes in high elevation stream nitrate dynamics. *Glob. Change Biol.* 15, 1777–1789.
- Beniston, M., 2003. Climatic change in mountain regions: a review of possible impacts. *Clim. Change* 59, 5–31.
- Berger, A., Loutre, M.F., 1991. Insolation values for the climate of the last 10 million years. *Quat. Sci. Rev.* 10, 297–317.
- Blaauw, M., 2010. Methods and code for 'classical' age-modeling of radiocarbon sequences. *Quat. Geochronol.* 5, 512–518.
- Blackwelder, E., 1915. Post-Cretaceous history of the mountains of central western Wyoming. *J. Geol.* 23, 97–117.
- Brozovic, N., Burbank, D.W., Meigs, A.J., 1997. Climatic limits on landscape development in the northwestern Himalaya. *Science* 276, 571–574.
- Brunelle, A., Whitlock, C.A., 2003. Postglacial fire, vegetation, and climate history in the Clearwater Range, Northern Idaho, USA. *Quat. Res.* 60, 307–318.
- Byrd, J.O., Smith, R.B., Geissman, J.W., 1994. The Teton Fault, Wyoming: topographic signature, neotectonics, and mechanisms of deformation. *J. Geophys. Res.* 99, 20,099–20,122.
- Byrd, J.O.D., 1994. Neotectonics of the Teton Fault. University of Utah, Wyoming, p. 295. Ph.D. dissertation.
- Colman, S.M., Pierce, K.L., 1981. Weathering rinds on Andesitic and Basaltic Stones as a Quaternary age indicator, Western United States. *U.S. Geol. Surv. Prof. Pap.* 1210, 56.
- Dahl, S.O., Bakke, J., Øyvind, L., Nesje, A., 2003. Reconstruction of former glacier equilibrium-line altitudes based on proglacial sites: an evaluation of approaches and selection of sites. *Quat. Sci. Rev.* 22, 275–287.
- Davis, P.T., 1988. Holocene glacier fluctuations in the American Cordillera. *Quat. Sci. Rev.* 7, 129–157.
- Davis, P.T., Gosse, J.C., Romito, M., Sorenson, C., Klein, J., Dahms, D., Zielinski, G., Jull, A.J.T., 1998. Younger Dryas Age for Type Titcomb Basin and Type Temple Lake Moraines, Wind River Range, Wyoming, USA. In: Geological Society of America Abstract with Programs, vol. 30, p. A-66.
- Denton, G.H., Karlén, W., 1973. Holocene climatic variations their pattern and possible cause. *Quat. Res.* 155–205.
- Dustin, J.S., Miller, A.W., 2001. Trophic state evaluation for selected lakes in Grand Teton National Park. *J. Am. Water Resour. Assoc.* 37, 887–898.
- Egholm, D.L., Nielsen, S.B., Pedersen, V.K., Lesemann, J.E., 2009. Glacial effects limiting mountain height. *Nature* 460, 884–887.
- Fenneman, N.M., 1931. Physiography of the Western United States. McGraw Hill, New York, p. 562.
- Finkenbinder, M.S., Abbott, M.B., Edwards, M.E., Langdon, C.T., Steinman, B.A., Finney, B.P., 2014. A 31,000 year record of paleoenvironmental and lake level change from Harding Lake, Alaska, USA. *Quat. Sci. Rev.* 87, 98–113.
- Foster, D., Brocklehurst, S.H., Gawthorpe, R.L., 2008. Small valley glaciers and the effectiveness of the glacial buzzsaw in the northern Basin and Range, USA. *Geomorphology* 102, 624–639.
- Foster, D., Brocklehurst, S.H., Gawthorpe, R.L., 2010. Glacial–topographic interactions in the Teton range, Wyoming. *J. Geophys. Res.* 115, F01007.
- Fryxell, F.M., 1935. . Glaciers of the Grand Teton National Park of Wyoming. *J. Geol.* 43, 381–397.
- Gardner, A., Moholdt, G., Cogley, J.G., Wouters, B., Arendt, A.A., Wahr, J., Berthier, E., Hock, R., Pfeffer, W.T., Kaser, G., Ligtenberg, S.R.M., Bolch, T., Sharp, M.J., Hagen, J.O., van den Broeke, M.R., Paul, F., 2013. A reconciled estimate of glacier contributions to sea level rise: 2003 to 2009. *Science* 340, 852–857.
- Gosse, J.C., Klein, J., Evenson, E.B., Lawn, B., Middleton, R., 1995a. Beryllium-10 dating of the duration and retreat of the last Pinedale glacial sequence. *Science* 268, 1329–1333.
- Gosse, J.C., Evenson, E.B., Klein, J., Lawn, B., Middleton, R., 1995b. Precise cosmogenic <sup>10</sup>Be measurements in western North America: support for a global Younger Dryas cooling event. *Geology* 23, 877–880.
- Hallet, B., Hunter, L., Bogen, J., 1996. Rates of erosion and sediment evacuation by glaciers: a review of field data and their implications. *Glob. Planet Change* 12, 213–235.
- Hallett, D.J., Hills, L.V., Clague, J.J., 1997. New accelerator mass spectrometry radiocarbon ages for the Mazama tephra layer from Kootenay National Park, British Columbia, Canada. *Can. J. Earth Sci.* 34, 1202–1209.
- Hampel, A., Hetzel, R., Densmore, A.L., 2007. Postglacial slip-rate increase on the Teton normal fault, northern Basin and Range Province, caused by melting of the Yellowstone ice cap and deglaciation of the Teton Range? *Geology* 35, 1107–1110.
- Hampel, H., Hetzel, R., 2008. Slip reversals on active normal faults related to the inflation and deflation of magma chambers: Numerical modeling with application to the Yellowstone-Teton region. *Geophys. Res. Lett.* 35, L07301.
- Heiri, O., Lotter, A.F., Lemcke, G., 2001. Loss on ignition as a method for estimating organic and carbonate content in sediments: reproducibility and comparability of results. *J. Paleolimnol.* 25, 101–110.
- Karlén, W., 1981. Lacustrine sediment studies: a technique to obtain a continuous record of Holocene glacier variations. *Geogr. Ann.* 63, 273–281.
- Kuehn, S.C., Froese, D.G., Carrara, P.E., Foit Jr., F.F., Pearce, N.J.G., Rotheisler, P., 2009. Major- and trace-element characterization, expanded distribution, and a new chronology for the latest Pleistocene Glacier Peak tephra in western North America. *Quat. Res.* 71, 201–216.
- Krause, T.R., Whitlock, C., 2013. Climate and vegetation change during the late-glacial/early-Holocene transition inferred from multiple proxy records from Blacktail Pond, Yellowstone National Park, USA. *Quat. Res.* 79, 391–402.
- Krause, T.R., Lu, Y., Whitlock, C., Fritz, S.C., Pierce, K.L., 2015. Patterns of terrestrial and limnologic development in the northern Yellowstone Ecosystem (USA) during the late-glacial/early-Holocene transition. *Paleoceanogr. Paleoclimatol. Paleocol.* 422, 46–56.
- Langdon, P.G., Leng, M.J., Holmes, M., Caseldine, C.J., 2010. Lacustrine evidence of early-Holocene environmental change in northern Iceland: a multiproxy paleoecology and stable isotope study. *The Holocene* 20, 205–214.
- Larsen, D.J., Miller, G.H., Geirsdóttir, Á., Thordarson, T., 2011. A 3000-year varved record of glacier activity and climate change from the proglacial lake Hvitárvatn. *Quat. Sci. Rev.* 30, 2715–2731.
- Larsen, D.J., Miller, G.H., Geirsdóttir, Á., Ólafsdóttir, S., 2012. Non-linear Holocene climate evolution in the North Atlantic: a high-resolution, multi-proxy record of glacier activity and environmental change from Hvitárvatn, central Iceland. *Quat. Sci. Rev.* 39, 14–25.
- Leonard, E.M., 1997. The relationship between glacial activity and sediment production: evidence from a 4450-year varve record of neoglaciation in Hector Lake, Alberta, Canada. *J. Paleolimnol.* 17, 319–330.
- Licciardi, J.M., Clark, P.U., Brook, E.J., Pierce, K.L., Kurz, M.D., Elmore, D., Sharma, P., 2001. Cosmogenic <sup>3</sup>He and <sup>10</sup>Be chronologies of the northern outlet glacier of the Yellowstone ice cap, Montana, USA. *Quat. Res.* 29, 1095–1098.
- Licciardi, J.M., Clark, P.U., Brook, E.J., Elmore, D., Sharma, P., 2004. Variable responses of western US glaciers during the last deglaciation. *Geology* 32, 81–84.
- Licciardi, J.M., Pierce, K.L., 2008. Cosmogenic exposure-age chronologies of Pinedale and Bull Lake glaciations in greater Yellowstone and the Teton range, USA. *Quat. Sci. Rev.* 27, 814–831.
- Lifton, N., Sato, T., Dunai, T.J., 2014. Scaling in situ cosmogenic nuclide production rates using analytical approximations to atmospheric cosmic-ray fluxes. *Earth Planet. Sci. Lett.* 386, 149–160.
- Love, J.D., Reed Jr., J.C., Christiansen, A.C., 1992. Geologic Map of Grand Teton National Park. U.S. Geological Survey Miscellaneous Investigations Series Map I-2031, Scale 1:62,500.
- Love, J.D., Reed Jr., J.C., Pierce, K.L., 2003. Creation of the Teton Landscape, a Geological Chronicle of Jackson Hole and the Teton Range. Grand Teton Natural History Association, Moose, Wyoming, p. 132.
- Machette, M.N., Pierce, K.L., McCalpin, J.P., Haller, K.M., Dart, R.L., 2001. Map and Data for Quaternary Faults and Folds in Wyoming, p. 153. U.S. Geological Survey Open File Report 01-461.
- Mahaney, W.C., 1975. Soils of post-Audubon age, Teton Glacier area. *Wyo. Arct. Alp. Res.* 7, 141–153.
- Mahaney, W.C., Spence, J., 1984. Glacial and periglacial sequence and floristics in the Jaw Cirque, central Teton Range, western Wyoming. *Am. J. Sci.* 284, 1056–1081.
- Maloney, J.M., Noble, P.J., Driscoll, N.W., Kent, G.M., Smith, S.B., Schmauder, G.C., Babcock, J.M., Baskin, R.L., Karlin, R., Kell, A.M., Seitz, G.G., Zimmerman, S., Kleppe, J.A., 2013. Paleoseismic history of Fallen Leaf segment of the West Tahoe–Dollar Point fault reconstructed from slide deposits in the Lake Tahoe Basin, California–Nevada. *Geosphere* 9, 1065–1090.
- Marrero, S.M., Phillips, F.M., Borchers, B., Lifton, N., Aumer, R., Balco, G., 2016. Cosmogenic nuclide systematics and the CRONUScal program. *Quat. Geochronol.* 31, 160–187.
- Marston, R.A., Weibs, B.J., Butler, W.D., 2011. Slope Failures and Cross-valley Profiles. University of Wyoming National Park Service Research Center, Grand Teton National Park, Wyoming, pp. 51–64. Annual Report 33.
- Menounos, B., Reasoner, M.A., 1997. Evidence for cirque glaciation in the Colorado Front range during the Younger Dryas chronozone. *Quat. Res.* 48, 38–47.

- Mensing, S., Korfmacher, J., Minckley, T., Musselman, R., 2012. A 15,000 year record of vegetation and climate change from a treeline lake in the Rocky Mountains, Wyoming, USA. *The Holocene* 22, 739–748.
- Meyers, P.A., Teranes, J.L., 2001. Sediment organic matter. In: Last, W.M., Smol, J.P. (Eds.), *Tracking Environmental Change Using Lake Sediments, Physical and Geochemical Methods*, vol. 2. Kluwer, Dordrecht, pp. 239–269.
- Millsapugh, S.H., Whitlock, C., Bartlein, P.J., 2004. Postglacial fire, vegetation, and climate history of the Yellowstone–Lamar and Central Plateau provinces, Yellowstone National Park. In: Wallace, L. (Ed.), *After the Fires: The Ecology of Change in Yellowstone National Park*. Yale University Press, pp. 10–28.
- Mitchell, S.G., Humphries, E.E., 2015. Glacial cirques and the relationship between equilibrium line altitudes and mountain range height. *Geology* 43, 35–38.
- Mortlock, R.A., Froelich, P.N., 1989. A simple method for the rapid determination of biogenic opal in pelagic marine sediments. *Deep Sea Res. Part A* 36, 1415–1426.
- Mote, P.W., Hamlet, A.F., Clark, M.P., Lettenmaier, D.P., 2005. Declining mountain snowpack in western North America. *Bull. Am. Meteorol. Soc.* <http://dx.doi.org/10.1175/BAMS-86-1-39>.
- Mumma, S.A., Whitlock, C., Pierce, K.L., 2012. A 28,000 year history of vegetation and climate from Lower Red Rock Lake, Centennial Valley, southwestern Montana. *Palaeogeogr. Palaeoclimatol. Palaeoecol.* 326–328, 30–41.
- Nelson, D.B., Abbott, M.B., Steinman, B., Polissar, P.J., Stansell, N.D., Ortiz, J.D., Rosenmeier, M.F., Finney, B.P., Riedel, J., 2011. Drought variability in the Pacific Northwest from a 6,000-yr lake sediment record. *Proc. Natl. Acad. Sci.* <http://dx.doi.org/10.1073/pnas.1009194108>.
- North Greenland Ice Core Project members, 2004. High-resolution record of northern hemisphere climate extending into the last interglacial period. *Nature* 431, 147–151.
- Phillips, F.M., Zreda, M.G., Goss, J.C., Klein, J., Evenson, E.B., Hall, R.D., Chadwick, O.A., Sharma, P., 1997. Cosmogenic <sup>36</sup>Cl and <sup>10</sup>Be ages of Quaternary glacial and fluvial deposits of the Wind River range, Wyoming. *Geol. Soc. Am. Bull.* 109, 1453–1463.
- Pickering White, B.J., Smith, R.B., Husen, S., Farrell, J.M., Wong, I., 2009. Seismicity and earthquake hazard analysis of the Teton–Yellowstone region, Wyoming. *J. Volcanol. Geotherm. Res.* 188, 277–296.
- Pierce, K.L., Obradovich, J.D., Friedman, I., 1976. Obsidian hydration dating and correlation of Bull Lake and Pinedale glaciations near West Yellowstone, Montana. *Geol. Soc. Am. Bull.* 87, 703–710.
- Pierce, K.L., 1979. History and dynamics of glaciation in the northern Yellowstone National Park area. *U.S. Geol. Surv. Prof. Pap.* 729F, 91.
- Pierce, K.L., Good, J.D., 1992. Field guide to the Quaternary geology of Jackson Hole, Wyoming, U.S. Geological Survey. Open File Rep. 92–504, 49.
- Pierce, K.L., 2003. Pleistocene glaciations of the Rocky Mountains. In: Gillespie, A.R., Porter, S.C., Atwater, B.F. (Eds.), *The Quaternary Period in the United States, Developments in Quaternary Science*, vol. 1. Elsevier, pp. 63–76.
- Pierce, K.L., Muhs, D.R., Fosberg, M.A., Mahan, S.A., Rosenbaum, J.G., Licciardi, J.M., Pavich, M.J., 2011. A loess–paleosol record of climate and glacial history over the past two glacial–interglacial cycles (~150 ka), southern Jackson Hole, Wyoming. *Quat. Res.* 76, 119–141.
- Porter, S.C., Pierce, K.L., Hamilton, T.D., 1983. Late Pleistocene glaciation in the Western United States. In: Porter, S.C. (Ed.), *The Late Pleistocene*, Vol. 1, of: Wright, H.E., Jr. (Ed.), *Late Quaternary Environments of the United States*. University of Minnesota Press, Minneapolis, MN, pp. 71–111.
- Pribyl, P., Shuman, B.N., 2014. A computational approach to Quaternary lake-level reconstruction applied in the central Rocky Mountains, Wyoming, USA. *Quat. Res.* 82, 249–259.
- Rasmussen, S.O., Andersen, K.K., Svensson, A., Steffensen, J.P., Vinther, B.M., Clausen, H.B., Siggaard-Andersen, M.L., Johnsen, S.J., Larsen, L.B., Dahl-Jensen, D., 2006. A new Greenland ice core chronology for the last glacial termination. *J. Geophys. Res. Atmos.* 111, D06102.
- Reasoner, M.A., Jodry, M.A., 2000. Rapid response of alpine timberline vegetation to the Younger Dryas climate oscillation in the Colorado Rocky Mountains, USA. *Geology* 28, 51–54.
- Reimer, P.J., Bard, E., Bayliss, A., Beck, J.W., Blackwell, P.G., Bronk Ramsey, C., Buck, C.E., Cheng, H., Edwards, R.L., Friedrich, M., Grootes, P.M., Guilderson, T.P., Haffidason, H., Hajdas, I., Hatté, C., Heaton, T.J., Heaton, T.J., Hoffmann, D.L., Hogg, A.G., Hughen, K.A., Kaiser, K.F., Kromer, B., Manning, S.W., Niu, M., Reimer, R.W., Richards, D.A., Scott, E.M., Southon, J.R., Staff, R.A., Turney, C.S.M., van der Plicht, J., 2013. *IntCal13 and Marine13 radiocarbon age calibration curves, 0–50,000 years cal BP*. *Radiocarbon* 55, 1869–1887.
- Roberts, S.V., Burbank, D.W., 1993. Uplift and thermal history of the Teton Range (north–western Wyoming) defined by apatite fission-track dating. *Earth Planet. Sci. Lett.* 118, 295–309.
- Rodbell, D.T., Seltzer, G.O., Mark, B.G., Smith, J.A., Abbott, M.B., 2008. Clastic sediment flux to tropical Andean lakes: records of glaciation and soil erosion. *Quat. Sci. Rev.* 27, 1612–1626.
- Saros, J.E., Rose, K.C., Clow, D.W., Stephens, V.C., Nurse, A.B., Arnett, H.A., Stone, J.R., Williamson, C.E., Wolfe, A.P., 2010. Melting alpine glaciers enrich high-elevation lakes with reactive nitrogen. *Environ. Sci. Technol.* 44, 4891–4896.
- Schachtman, N.S., MacGregor, K.R., Myrbo, A., Hencir, N.R., Riihimaki, C.A., Thole, J.T., Bradtmiller, L.L., 2015. Lake core record of Grinnell Glacier dynamics during the latest Pleistocene deglaciation and the Younger Dryas, Glacier National Park, Montana, USA. *Quat. Res.* 84, 1–11.
- Settele, J., Scholes, R., Betts, R., Bunn, S., Leadley, P., Nepstad, D., Overpeck, J.T., Taboada, M.A., 2014. Terrestrial and inland water systems. In: Field, C.B., Barros, V.R., Dokken, D.J., Mach, K.J., Mastrandrea, M.D., Bilir, T.E., Chatterjee, M., Ebi, K.L., Estrada, Y.O., Genova, R.C., Girma, B., Kissel, E.S., Levy, A.N., MacCracken, S., Mastrandrea, P.R., White, L.L. (Eds.), *Climate Change 2014: Impacts, Adaptation, and Vulnerability. Part a: Global and Sectoral Aspects. Contribution of Working Group II to the Fifth Assessment Report of the Intergovernmental Panel on Climate Change*. Cambridge University Press, Cambridge, United Kingdom and New York, NY, USA, pp. 271–359.
- Sharp, W., Ludwig, K.R., Chadwick, O.A., Amundson, R., Glaser, L.L., 2003. Dating fluvial terraces by <sup>230</sup>Th/U on pedogenic carbonate, Wind River Basin, Wyoming. *Quat. Res.* 59, 139–150.
- Shaw, R.J., 2000. *Plants of Yellowstone and Grand Teton National Parks*. Wheelwright Publishing, Salt Lake City, UT, p. 159.
- Shuman, B., Henderson, A.K., Colman, S.M., Stone, J.R., Fritz, S.C., Stevens, L.R., Power, M.J., Whitlock, C., 2009. Holocene lake-level trends in the Rocky Mountains, USA. *Quat. Sci. Rev.* 28, 1861–1879.
- Shuman, B., Pribyl, P., Minckley, T.A., Shinker, J.J., 2010. Rapid hydrologic shifts and prolonged droughts in Rocky Mountain headwaters during the Holocene. *Geophys. Res. Lett.* 37, L06701.
- Slemmons, K.E.H., Saros, J.E., 2012. Implications of nitrogen-rich glacial meltwater for phytoplankton diversity and productivity in alpine lakes. *Limnol. Oceanogr.* 57, 1651–1663.
- Smith, R.B., Byrd, J.O.D., Susong, D.D., 1993. Seismotectonics, Quaternary history, and earthquake hazards of the Teton fault, Wyoming. In: Snoke, A., Steidmann, J.R., Roberts, S. (Eds.), *Geology of Wyoming*, Mem. vol. 5. Geological Society of Wyoming, Laramie, pp. 628–667.
- Stuiver, M., Reimer, P.J., Reimer, R.W., 2005. CALIB 6.0 WWW Program and Documentation.
- Talbot, M.R., 2001. Nitrogen isotopes in paleolimnology. In: Last, W.M., Smol, J.P. (Eds.), *Tracking Environmental Change Using Lake Sediments, Physical and Geochemical Methods*, vol. 2. Kluwer, Dordrecht, pp. 401–439.
- Thackray, G.D., Lundeen, K.A., Borgert, J.A., 2004. Latest Pleistocene alpine glacier advances in the Sawtooth Mountains, Idaho, USA: reflections of midlatitude moisture transport at the close of the last glaciation. *Geology* 32, 225–228.
- Thackray, G.D., 2008. Varied climatic and topographic influences on late Pleistocene mountain glaciation in the western United States. *J. Quat. Sci.* 23, 671–681.
- Thackray, G.D., Staley, A.E., 2014. Extensive glaciation during MIS 4 and 3 in the Teton range, Wyoming. *Geol. Soc. Am. Abstr. Programs* 46, 41.
- Tranel, L.M., Spotila, J.A., Kowalewski, M.J., Waller, C.M., 2011. Spatial variation of erosion in a small, glaciated basin in the Teton Range, Wyoming, based on detrital apatite (U–Th)/He thermochronology. *Basin Res.* 23, 571–590.
- Tranel, L.M., Spotila, J.A., Binnie, S.A., Freeman, S.P.H.T., 2015. Quantifying variable erosion rates to understand the coupling of surface processes in the Teton Range, Wyoming. *Geomorphology* 228, 409–420.
- Vinther, B.M., Clausen, H.B., Johnsen, S.J., Rasmussen, S.O., Andersen, K.K., Buchardt, S.L., Seierstad, I.K., Siggaard-Andersen, M.L., Steffensen, J.P., Svensson, A.M., Olsen, J., Heinemeier, J., 2006. A synchronized dating of three Greenland ice cores throughout the Holocene. *J. Geophys. Res.* 111, D13102.
- Walther, G.R., Post, E., Convey, P., Menzel, A., Parmesan, C., Beebee, T.J., Fromentin, J.M., Hoegh-Guldberg, O., Bairlein, F., 2002. Ecological responses to recent climate change. *Nature* 416, 389–395.
- Westerling, A.L., Hidalgo, H.G., Cayan, D.R., Swetnam, T.W., 2006. Warming and earlier spring increase western U.S. forest wildfire activity. *Science* 313, 940–943.
- Whitlock, C., 1993. Postglacial vegetation and climate of Grand Teton and southern Yellowstone National Parks. *Ecol. Monogr.* 63, 173–198.
- Whitlock, C., Bartlein, P.J., 1993. Spatial variations of Holocene climatic change in the Yellowstone region. *Quat. Res.* 39, 231–238.
- Whitlock, C., Dean, W., Rosenbaum, J., Stevens, L., Fritz, S., Bracht, B., Power, M., 2008. A 2650-year-long record of environmental change from northern Yellowstone National Park based on a comparison of multiple proxy data. *Quat. Int.* 188, 126–138.
- Whitlock, C., Dean, W.E., Fritz, S.C., Stevens, L.R., Stone, J.R., Power, M.J., Rosenbaum, J.R., Pierce, K.L., Bracht-Flyer, B.B., 2012. Holocene seasonal variability inferred from multiple proxy records from Crivice Lake, Yellowstone National Park, USA. *Paleogeogr. Paleoclimatol. Paleocool.* 331–332, 90–103.
- Williams, M.W., Knauf, M., Cory, R., Caine, N., Liu, N., 2007. Nitrate content and potential microbial signature of rock glacier outflow, Colorado Front Range. *Earth Surf. Process. Landf.* 32, 1032–1047.
- Young, N.E., Briner, J.P., Leonard, E.M., Licciardi, J.M., Lee, K., 2011. Assessing the climatic and nonclimatic forcing of Pinedale glaciation and deglaciation in the western United States. *Geology* 39, 171–174.
- Young, N.E., Briner, J.P., Rood, D.H., Finkel, R.C., 2012. Glacier extent during the Younger Dryas and the 8.2-ka event on Baffin Island, Arctic Canada. *Science* 337, 1330–1333.
- Zhang, P., Molnar, P., Downs, W.R., 2001. Increased sedimentation rates and grain sizes 2–4 Myr ago due to the influence of climate change on erosion rates. *Nature* 410, 891–897.
- Zielinski, G.A., Davis, P.T., 1987. Late Pleistocene age of the type Temple Lake moraine, Wind River range, Wyoming, USA. *Geogr. Phys. Quat.* 41, 397–401.
- Zdanowicz, C.M., Zielinski, G.A., Germani, M.S., 1999. Mount Mazama eruption: Calendrical age verified and atmospheric impact assessed. *Geology* 27, 621–624.